FURTHER DEVELOPMENT AND IMPLEMENTATION OF AN EU-LEVEL FOREST MONITORING SYSTEM
- FUTMON-

ACTION: D1: *TREE VITALITY AND ADAPTATION*

IN COOPERATION WITH THE INTERNATIONAL COOPERATIVE PROGRAMME ON ASSESSMENT AND MONITORING OF AIR POLLUTION EFFECTS ON FORESTS (ICP FORESTS)

Final report D1 (A D1 10)

Part 2: Report on methods to assess Leaf Area Index (LAI) including LIDAR

Elaborated by: Stefan Fleck, Inga Mölder and Johannes Eichhorn

Northwest German Forest Research Station
37079 Göttingen, Grätzelstr. 2
Germany

Part 2: Report on methods to assess Leaf Area Index (LAI) including LIDAR

Part 2[1]

[1] **Note**: Final report D1 (A D1 10) includes two parts:
Part 1: Tree vitality and adaptation
Part 2: Report on methods to assess Leaf Area Index (LAI) including LIDAR

2 *Introduction*

2.1 Objectives of the current study

The assessment of the vitality status of forests employs the measurement of defoliation as one of the most important indicators for tree vitality. Defoliation is measured by assessments on sample trees of Kraft classes 1 to 3 and here selectively on the uppermost part of the crown, since growth and foliage density of this sun-exposed upper part of the crown are of outstanding importance for the trees' physiology and their competitive success.
Obviously, the defoliation rating for this part of the canopy may not provide a satisfying description of amount and distribution of all leaves in a forest due to its selective nature. The whole canopy comprises trees of all Kraft classes and naturally includes shaded and lower parts of the tree crowns, which all contribute to the total leaf area and its distribution. But it is especially this information that would be valuable for process models of the canopy which are based on light or water penetration through foliage, particle deposition on leaf surfaces, or CO_2-uptake by leaves. Due to its importance the parameter LAI receives an increasing awareness in the monitoring measures. A new part of the ICP-Forests manual will tackle methodological recommendations in order to use Plant Canopy Analyzers in a harmonized way.

The total amount of leaves is given by the leaf area index (LAI). LAI is defined as half the total surface area of leaves in the canopy per ground area (Chen and Black 1991). A wide range of measurement methods is available for LAI-determination (Jonckheere et al. 2004), including the direct measurement with litter traps and sampling of specific leaf area as well as indirect methods that are based on gap fraction measurement with optical devices. While the laborious litter trap method is still regarded as the most reliable assessment for intensive monitoring plots, gap-fraction based methods like the Plant Canopy Analyzer LAI-2000 (PCA), TRAC, or hemispherical photographs are considered to deliver repeatable approximations up to a leaf area index of 5 or 6, while higher LAIs correspond to so small gap fractions that the methods get unreliable (Jonckheere et al. 2004). PCA and the other indirect methods employ the exponential function between light penetrating through canopy gaps and the projected area of canopy elements (leaves, branches, fruits, flowers) in an assumed homogenous spatial distribution of these elements in the canopy that allows to use the Beer-Lambert law (Monsi and Saeki 1953).

Certain methodological constraints are given for the optical determination of gap fractions with the PCA in order to use them for LAI derivation on monitoring plots:

- The measurement has to be performed under overcast sky conditions. Alternatively, the measurement can be performed pre-dawn or after sunset, so that no direct sunlight impairs the PCA-readings.
- A nearby clearing must be available for above canopy measurements with a second PCA-sensor. The opening angle in the centre of the clearing must be at least 120°.
- The PCA-sensor can not be used directly under a leaf or branch.
- The measurement is repeated 16 times along a regular grid of points in order to get a spatially representative average.
- The contribution of woody surfaces to the measurement needs to be estimated, requiring an additional PCA-measurement in winter (only deciduous trees).
- A correction for the clumped distribution of leaves needs to be performed based on additional measurements with the TRAC device or hemispherical photographs.

The following study compares direct litter-trap measurements of LAI with indirect methods based on gap fraction assessments with the PCA and LIDAR devices (airborne and terrestrial laser-scanning, ALS and TLS) and is focussed on 5 main questions:

1. Litter-trap measured LAI is used as best approximation to the real amount of leaf area. To what extent is this confirmed by LIDAR measurements (ALS and TLS)?
2. How need PCA measurements to be evaluated in order to fit best to the litter trap measurements?
3. Which PCA-derived indices fit best to ALS and TLS measurements?
4. How are indicators of the crown condition assessment related to the different kinds of LAI assessment?
5. Which recommendations can be derived for the best possible PCA-configuration in view of harmonized procedures of the European Forest Monitoring. Which methods should be included in the new ICP-forests Manual on LAI measurements?

2.2 Relationships between crown measures for tree health and LAI

The similarity of gap fraction with the amount of visible sky needed for crown transparency measurements might lead to the impression that gap fraction based measurements of LAI must be somehow related to crown transparency. Smolander et al. (2000) investigated this relationship, but the coefficient of determination for 8 pine stands (r^2=0.52) and 20 measurements in spruce stands (r^2=0.36) was quite low, so that the hope to replace crown transparency measurements with PCA-measurements could not fulfill. Apart from the selective nature of crown transparency measurements, this may also be attributed to the different view angle of both measurements, since the PCA measurements include the whole canopy and all view angles from zenith to 74°, while crown transparency and defoliation measurements include only a section of the upper part of single crowns and a view angle of about 45° depending on spatial arrangement of the trees.

The correlation between crown transparency and defoliation was shown to be close (R^2= 0.88) for one *Quercus ilex* stand in the investigation of Bussotti et al. (2003), while it was low for the other stand (R^2= 0.12). The defoliation values were always higher than the transparency values, which could be explained by a similar type of relationship between both quantities as the one between gap fraction and projected area of canopy elements in indirect LAI measurements. But also other aspects like the explicit non-consideration of flowers in the defoliation assessment may lead to different trends in both quantities. Nevertheless, both quantities were reasonably correlated to the mass of shed leaves measured by litter traps (r^2=0.71 and 0.42, respectively), so that temporal changes of the amount of foliage may well and similarly be reflected by both quantities.

The obvious difference between LAI and crown condition measurements that is due to the selection of different parts of the canopy may not be further investigated with ground-based PCA-measurements, since the PCA-measured gap fraction does always include lower and upper canopy. Only 3-D-measurements like the employed LiDAR measurements may be evaluated separately for different parts of the canopy.

Airborne and terrestrial LiDAR (Light Detection And Ranging) are methods that do not directly measure leaf area index or light transmission, the measurement is based on the localization of laser beam-reflecting biomass with distance and angle measurements. While airborne LiDAR is executed in a usually lower resolution from the upper side of the canopy, terrestrial LiDAR uses the same measurement principle from beneath the canopy with much higher resolution. 3D-crown reconstructions based on terrestrial LiDAR often look like a natural tree, though the uppermost part of the crown is usually given in lower resolution (Fleck et al. 2011). The potential of airborne LiDAR for 3D-crown reconstruction is especially high, when full waveform LiDAR is used. Full waveform LiDAR results in several localized reflections from a single laser shot, and thereby delivers a higher point density. With regard to the definition of defoliation and crown transparency, airborne laser scanning (ALS) is a promising measurement principle, since it measures best in the uppermost part of the crown.

3 *Detailed technical description of Action C1-TREE-30*

3.1 Compared measurement methods

An overview of the different measurement methods compared in this study is given in table 1 and their technical background is explained in this section, while the implementation of the techniques in our field study is described in section 3.2: Field measurements.

3.1.1 Leaf litter collections

Given that the whole leaf area of a forest stand falls down to the forest floor at the end of the vegetation period, the measured one-sided area of leaf litter per unit ground area represents the LAI of this stand in the definition of Chen and Black (1992). To measure it for the whole stand, the leaf litter may be sampled from the floor with a number of litter traps of known area that is adequate to represent the spatial variability of leaf area on the floor. Repeated emptying over the leaf-fall period is necessary to avoid leaf decomposition before the leaves are measured. In order to avoid leaf area measurements on every leaf, leaf samples may be taken from each litter trap and their specific leaf area (SLA, leaf area per dry weight) determined, so that the leaf area in a litter trap may be calculated from dry weight determination of leaf litter and multiplication with SLA. Since no further correction is necessary, LAI_L, the litter trap-based LAI, serves as reference measurement against which other methods of LAI-determination may be evaluated.

3.1.2 Plant Canopy Analyzer LAI-2000 (PCA)

The Plant Canopy Analyzer (LAI-2000; Li-Cor, Lincoln, Nebraska, USA) is an instrument to measure blue diffuse light (below 490nm wavelength). Fisheye optics is integrated to project a hemispherical image onto five detectors which measure radiation intensities in five concentric fields of view. The five sensors are centred at zenith angles θ of 7°, 23°, 38°, 53° and 68°, respectively. Simulataneously aquired above-canopy (A-) and below-canopy (B-) readings are required to obtain the gap fraction, which represents the probability of diffuse light non-inteceptance for each zenith angle (GF(θ)).

The leaf area index (LAI) calculation for this and other optical instruments is based on an inversion of the exponential relationship between LAI and light penetration that may be derived from the Beer-Lambert law for light transmittance through a solution. Analogously to extinction coefficient, absorber concentration, and path length in the Beer-Lambert law, light penetration through the canopy is dependent on foliage orientation (given as relative projected leaf area in beam direction, G(θ)), volumetric leaf area density (μ) and path length of the

Table 1:

Measured parameter	**Abbrevation**	**Different calculations according to**	**Method**	**# of plots**
Litter trap-based leaf area index	LAI_L	-	Litter trap, SLA measurement	10
PCA-based leaf area index - corrected for clumping and for wood area index -	$LAI_{PCA}1$ to $LAI_{PCA}5$	**Used opening angle:** 1 ring of the PCA hemispherical sensor corresponds to an opening angle of 13°, 2 rings correspond to 28°, 3 rings correspond to 43°, 4 rings correspond to 58°, 5 rings correspond to 74°. **Summer and winter measurements** (with and without leaves)	PCA (leaf-on and leaf-off), TRAC	40
PCA-based gap fraction	$GF_{PCA}3$ to $GF_{PCA}5$		PCA in leaf-on condition	40
PCA-based effective leaf area index - raw instrument output -	$Le_{PCA}1$ to $Le_{PCA}5$ $Le_{PCA}1$winter to $Le_{PCA}5$winter		PCA in leaf-on condition	40
PCA-based total plant area index - instrument output corrected for clumping -	$Lt_{PCA}1$ to$Lt_{PCA}5$		PCA in leaf-on condition and TRAC for clumping coefficient	40
ALS-based gap fraction	GF_{ALS}F GF_{ALS}F+L GF_{ALS}All $GF_{ALS,upper}$ F $GF_{ALS,upper}$ F+L $GF_{ALS,upper}$ All	**Number of echoes considered**: F = First echo of each pulse F+L = First and last echo of each pulse All = All echoes of each pulse **Upper and lower canopy**	ALS	40
ALS-based plant area index	L_{ALS}F L_{ALS}F+L L_{ALS}All $L_{ALS,upper}$ F $L_{ALS,upper}$ F+L $L_{ALS,upper}$ All			
TLS-based gap fraction	$GF_{TLS}10$ to $GF_{TLS}50$	**Voxel size**: 10cm edge length to 50cm edge length **Upper and lower canopy**	TLS	30
TLS-based plant area index	$L_{TLS}10$ to $L_{TLS}50$		TLS	40
Mean tree-wise defoliation per plot	Defoliation	-	Visual assessment	40
Crown diameter related distance to neighbours	CDRD	-	Distance measurement	40
Fruiting, percentage of trees with medium or strong fructification	Fruiting	-	Visual classification	40
Apical shoot architecture	ROLOFF	-	Visual classification	40

beam through the canopy (S(θ)) (Monsi & Saeki 1953):

$$GF(\theta) = \exp[\,-G(\theta)\ \mu\ S(\theta)\,] \tag{1}$$

The conversion of GF(θ) into the theoretical contact number of a beam through the canopy in the given direction (LI-COR, inc. 1992) allows to use the exact solution of equation (1) for leaf area density as given by Miller (1967),

$$\mu = -2\int_0^{\pi/2} [\ln (GF(\theta))/\ S(\theta)] \sin(\theta)\, d\theta \tag{2}$$

which finally leads to an estimation of the effective leaf area index (L_e):

$$L_e = -2\int_0^{\pi/2} \ln (GF(\theta)) \cos(\theta) \sin(\theta)\, d\theta \tag{3}$$

where θ is the zenith angle ranging from 0 to π/2 and GF the gap fraction. L_e is here derived by multiplying μ with canopy height, assuming that the distribution of leaves in space is random. The term "effective LAI" (Chen et al. 1997) was introduced with respect to the fact that optical LAI-measurement instruments are able to measure this quantity, but not the LAI in the definition of Chen and Black (1991), since the assumption of random leaf distribution is usually not fulfilled due to leaf clumping and since leafy and non-leafy canopy elements are not distinguished in the measurement, so that surfaces of branches and fruits contribute to the measured effective index.

Based on the above and below canopy measurements in the 5 concentric rings of the PCA, L_e is calculated as

$$L_e = 2\sum_{i=1}^{5} \ln\left(\frac{I_a}{I_b}\right) \cos(\theta_i) w_i \tag{4}$$

, where I_a and I_b are the light intensity values measured above and below the canopy and the w_i are weights given for each of the five rings corresponding to sin(θ)dθ, where sin(θ) is the sine of the center angle of ring i and dθ is the range of angles covered by that ring.

The PCA-measurement needs still to be corrected for leaf clumping, since the non-randomness of leaf distribution in space causes higher gap fraction values than in the assumed random distribution and therefore an underestimation of LAI. The non-randomness is described as clumping coefficient Ω. Due to the absence of within shoot clumping in the case of broadleaved trees (LeBlanc et al. 2002), Ω can directly be derived from the between-shoot clumping index, which can be retrieved from gap size measurements with the TRAC instrument (Chen et al. 2006). The correction yields the total plant area index (L_t) as defined by Chen (1996):

$$L_t = L_e / \Omega \tag{5}$$

L_t may finally be converted to LAI in the definition of Chen and Black (1992) based on an estimation of the woody to total plant area ratio (α), which may be achieved by PCA measurements in the leafless state in winter:

$$\mathrm{LAI_{PCA}} = L_t\,(1\text{-}\alpha) \tag{6}$$

3.1.3 Airborne laser scanning (ALS)

Airborne and terrestrial LiDAR (Light Detection And Ranging) are methods that do not directly measure leaf area index or light transmission but localize canopy elements. The localization is based on distance and angle measurements of a laser beam and its reflections from material in and below the canopy. With regard to the definition of defoliation and crown transparency, airborne laser scanning (ALS) is a promising measurement principle, since it measures best in the uppermost part of the crown.

Airborne laser scanning is executed from a plane or helicopter whose position and orientation in space is permanently recorded with high accuracy using an inertial measurement unit. A laser beam is emitted to the ground and the timing of reflections from each shot is recorded to calculate distance to the reflecting objects based on speed of light. The footprint of the laser beam is typically larger than the canopy elements so that multiple reflections (called “echoes” or “pulses”) from different surfaces are possible. The reflections are visible as pulses in the waveform of the reflected signal and especially full waveform ALS systems are able to record all of the multiple returns. The final result of an (airborne or terrestrial) laser scan is a three-dimensional map of object positions in the surveyed area which is termed 3D point cloud.

In analogy to the gap fraction measurement of PCA, it is possible to derive the gap fraction of the canopy based on the proportion of laser beams penetrating the canopy (=ground reflections) in the total dataset. For this, a cutoff height needs to be defined to distinguish canopy reflections from ground reflections. Under the condition, that the laser beam angles employed were close to vertical, an ALS-based plant area index (L_{ALS}) may then be calculated as logarithm of the ratio between total number of echoes in the stand (N_{all}) and below canopy echoes:

$$\boldsymbol{L_{ALS}} = \text{Ln}\,(N_{all} / N_b) \tag{7}$$

The angular correction included in equations (3) and (4) is not performed here assuming vertical laser beams. The original formulation by Solberg et al (2006) additionally includes the division by an empirically derived coefficient k, which is necessary to account for effects of leaf orientation and leaf clumping and needs to be built on the regression to local LAI measurements. However, k does not consider the contribution of woody canopy elements to the measured index. We don’t perform this step here in order to compare the used methods without influence of possible biases introduced by any other method and keep in mind that the absolute values of L_{ALS} do, therefore, not necessarily lie in the same range as those from LAI_{PCA} or LAI_L.

3.1.4 Terrestrial laser scanning (TLS)

While airborne LiDAR is executed in a usually lower resolution from the upper side of the canopy with more or less vertical laser beams, terrestrial LiDAR uses the same measurement principle from beneath the canopy with much higher resolution and polar beam angle distribution, analogous to the projection of hemispherical images. In fact, a 360° x 180° terrestrial LiDAR scan equals a hemispherical picture in which the distance from the scanning position to each photo-pixel is known. The derivation of gap fractions and their evaluation to LAI-values is therefore possible in the same way as with other optical devices (e.g. PCA), when the scans are treated like hemispherical images (Danson et al. 2007, Moorthy et al. 2008).

The justification for this elaborate system comes from the additional information content in the unique 3D-description of trees it may deliver based on the combination of several high-resolution scans. The resulting 3D-reconstructions often look like a natural tree, though the uppermost part of the crown is mostly represented in lower resolution (Fleck et al. 2011).

Terrestrial laser scans in forests are usually executed with 3D-laser-scanners that are stationary and subsequently send laser beams into all possible azimuthal and elevational directions, thereby scanning their environment. Since they are stationary and the laser beams don’t penetrate the objects they hit, sight is blocked whenever an object is larger than the usually very small footprint of the laser beam. Therefore, multiple laser-scans from carefully selected positions need to be combined in order get a complete 3D-map of the objects in a forest. The combination of multiple scans is achieved via targets fixed in the scene that serve as control points for the coordinate transformation from one scan into the coordinate system of another scan.

The resulting combined 3D point cloud is principally similar to the 3D point cloud produced by ALS-systems, but it needs a different form of evaluation, since the laser beams are not vertically oriented and the 3D point cloud, therefore, has a density trend with the majority of points in the lower part of the point cloud. The density trend can be removed by transformation of the 3D point cloud to a voxel model consisting of equally spaced volume elements (voxels, i.e. cubes of the same width; Mariano et al. 2011). The voxels are either filled with canopy surfaces whenever there are canopy reflections in this part of the 3D point cloud or empty, when no reflection is recorded in the space represented by a certain voxel.

The voxel model has the disadvantage that it lowers the resolution of the information content of the original 3D point cloud, but it provides a new sort of canopy description that is distinct from other approaches. Taken as a rough model of the canopy, a TLS-based gap fraction (GF_{TLS}) may be extracted. GF_{TLS} is the proportion of gaps in a vertical projection of all voxels and is calculated from the proportion of total plot area (A_{total}) covered by canopy voxels (A_{Va}):

$$GF_{TLS} = 1 - A_{Va} / A_{total} \quad (8)$$

A TLS-based plant area index (L_{TLS}) has here been derived after (Fleck and Mölder 2011) based on GF_{TLS} and path length through the canopy (S, equaling average canopy height) as

$$L_{TLS} = -\mathrm{Ln}\,(GF_{TLS} / S) \quad (9)$$

3.2 Field measurements

3.2.1 Study areas

We established 20 plots with a size of 50 by 50m in each of two study areas, where we conducted comprehensive field measurements.

The study areas Krofdorf and Reinhardswald lie in the federal state of Hesse in Germany. The Krofdorf forest (18 km², 50.658° North, 8.653° East) contains all analysed beech stands and is situated 11 km northwest of Gießen and between 240 and 325 m above sea level (Voll 2001). Its mean annual temperature is 8.7°C (Deutscher Wetterdienst Offenbach, Germany, 2007) and the mean annual precipitation 696 mm per year for the period 1961-1990 (DWD, 2006). The climate can be described as slightly sub-continental. The parent rock material consists of argillite and greywacke with loess loam. Krofdorf belongs to the lower beech-mixed forest zone and the most frequent tree species in our study area is beech (Fagus sylvatica L.) followed by oak (Quercus spec.) In the majority of cases the Krofdorf forest consists of Cambisols and Lessivés and occasionally Stagnosols (Voll 2001).

The Reinhardswald (60 km², 51.487° North, 9.519° East) contains all analyzed oak stands and is situated on the north-eastern border of the Kassel Bassin. Its mean annual temperature is 7°C (DWD, 2007) and the mean annual precipitation at 756 mm per year for the period 1961 till 1990 (DWD, 2006). Middle sandstone with loess loam forms the parent rock material. The dominating tree species in our study area is oak followed by beech. Generally the Reinhardswald consists of Lessivés and Stagnosols (Neuhaus 1973). Stand age ranged from 23 to 155 for beech and from 15 to 203 for oak stands (compare Fig. 34).

3.2.2 Litter trap measurements

On 5 plots per study area, leaf area index was measured directly by leaf litter collection. The leaves were collected every 2 or 4 weeks during the leaf fall period 2009/2010 in 12 litter traps (surface area 0.207 m²) that were randomly distributed along grid cells on each plot (Fig. 1). Directly after sampling, the leaf area was measured for a subsample of 17 leaves with a flatbed scanner (CanoScan LiDE 200, Canon, Germany) and the software WinFOLIA (Regent Instruments, Canada). Afterwards, the subsamples were dried at 60°C and their dry weight was determined. By multiplying SLA (m^2/g) with the dry weight per litter trap area (g/m^2) we obtained the dimensionless leaf area index and averaged it to determine LAI_L.

3.2.3 PCA and TRAC measurements

PCA-measurements have been performed from July till mid of Septemger 2009 on all 20 plots of each study area. We worked with two sensors of the PCA: one sensor was used below the canopy in the stand; the other sensor acquired every 15 sec reference data on a clearance close to the studied plot. On each study plot, we took 16 measurements at 1.5 m under diffuse light conditions (overcast sky, dusk or dawn) along a regular grid (Fig. 1).

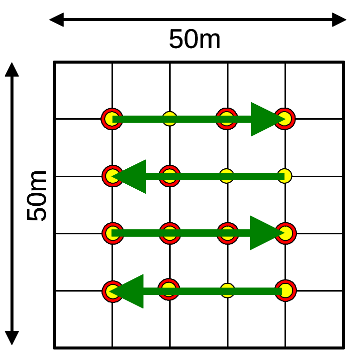

Fig. 1: Exemplary plot design. The 16 yellow dots mark positions for measurements with the Plant Canopy Analyzer, red circles stand for the 12 randomly distributed litter traps, the green arrows represent the transect of 120m measured with the TRAC device.

With the help of a 90° view cap on the sensor, the appearance of the operator on the hemispherical image was prohibited. Since both sensors were equipped with the same view cap, the operator always needed to measure in the same compass direction (B reading) as the reference sensor (A reading) on the clearance.

The between-shoot clumping factor $\Omega_,$ was measured with TRAC (Tracing Radiation and Architecture of Canopies, (Chen et al. 1997) on a transect of 120m (Fig. 1). An estimation of the woody to total plant area ratio α was achieved by PCA-measurements on 34 plots in the leafless state in winter 2010/2011. For 6 plots, α has been estimated from measurements in a similar stand nearby.

3.2.4 ALS measurements

Full waveform ALS-measurements were carried out on July 9th and 10th 2009. The airborne scans were done in a height of 300m with the TopEye system S/N 724 installed on a helicopter (SE-JIH). With a pulse frequency of 170kHz, a scanning frequency of 70Hz, and a maximum scan angle of ±12°, this resulted in a mean pulse density of about 60 returns per square meter. The xyz-data was classified into digital elevation model and digital surface model. In analogy to the LAI-2000 measurements, the cut-off level for the distinction of canopy echoes (N_a) from below canopy echoes (N_b) was set to 1.5m above ground.

Additional to the unweighted L_{ALS} after equation (7), three different sorts of echoes were evaluated separately: first echoes (L_{ALS}F), first and last echoes (L_{ALS}F+L) and all recorded echoes (L_{ALS}All) were used for L_{ALS} calculation. In the case of L_{ALS}F the first echo from each laser impulse was counted to derive N_{all} and N_b. For L_{ALS}F+L and L_{ALS}All echo counts were weighted relative to the total number of echoes belonging to their laser impulse (Solberg et al. 2009). L_{ALS}F+L was calculated by weighting first and last echoes with 0.5 and by weighting pulses which only gave a single echo with 1. A pre-study showed that the relationship between measurements of LAI-2000 and ALS got worse with increasing cutoff-height, except from stands with a dense layer of bracken (*Pteridium aquilinum*) (data not presented).

In addition to L_{ALS}, which is the result of gaps penetrating the whole canopy higher than 1.5m above ground, we calculated a separate airborne effective LAI for the upper ($L_{ALS,\ upper}$) and lower part of the canopy ($L_{ALS,\ lower}$). The boundary height between upper and lower canopy was chosen from histograms with a resolution of 0.1m of the tree height model (0.5m x 0.5m grid) of every plot and set to the most abundant value of the tree height model, which we assume to be the boundary between shaded and sunlit crown.

3.2.5 TLS measurements

The terrestrial laser scanner used was the Imager 5006 (Zoller + Fröhlich GmbH, Germany). It uses the phase difference method for distance measurements up to 79 m. The field of view envelops 360 x 310° and the maximum scanning speed is 500,000 pixels per second. We scanned with a high resolution of 10,000 x 10,000 pixels per 360° in both directions (Imager 5006 Manual, Zoller + Fröhlich GmbH 2010).

The scans were carried out from end of July till mid-September 2009 in both study areas with 15 beech plots in Krofdorf and 15 oak plots in the Reinhardswald. Scanning of the same plots was repeated from July till end of August 2010. 30 targets per plot were placed in different heights: at the foot of a tree, in approximately two meter height and up to 10 m height with telescopic rods in order to distribute targets to all regions of the scanned space. The targets had a chessboard pattern and were differentiable via combinations of numbers and/or letters. The scanner was placed at about 20 different positions per stand in order to take multiple scans.

The common control points of each two scans were registered and coordinate transformations calculated in the software Z+F LaserControl. The occurring deviations due to measurement errors were distributed via bundle-adjustment with the NEPTAN-program to optimize the coordinate transformation. Unwanted pixels in the scans were removed using 6 different filters with the following settings: thin filter for wavelengths >0.001m, single pixel filter (<2 pixels), mixed pixel filter (6 pixels, 2°), range filter (0.5-80m), intensity filter (0.6-100%) and invalidate filter (25°). The coordinate-transformed 3D point clouds were unified to one large 3D point cloud with a point cloud reduction of 1/cm (software Cyclone, Leica Geosystems, Switzerland).

The plot space was extracted from the unified 3D-point cloud and transformed to voxel models of different edge length: 10, 20, and 50cm. A threshold value of 5 points per voxel was chosen to consider a voxel as filled. In analogy to the PCA-measurements, all voxels above the cut-off level of 1.5m were considered as canopy voxels. They were identified based on a digital terrain model that was built on the lowest points per 50cm grid cell.

3.2.6 Crown condition measurements

The regular assessment of crown condition comprises apical shoot architecture (ROLOFF), crown defoliation, fruiting, and crown diameter related distance to tree neighbors (CDRD). These four assessments were performed on all 40 plots, investigating 32 trees per plot or – if there were less trees – on all trees of the plot. Average values were calculated and taken as representative for the investigated plot. In the case of fruiting, the relative proportion of trees with medium to high fructification (classes common and abundant) has been calculated. The measurements were performed according to the ICP-Forest manual.

Since ROLOFF, defoliation, and fruiting are related to only the upper part of the canopy, the comparison to L_{TLS} and L_{ALS} was supplemented by a comparison to $L_{TLS,upper}$ and $L_{ALS,upper}$, representing the same quantities selectively calculated for the upper part of the canopy. The subdivision into upper crown and lower crown was executed as follows: We measured the height of the tree canopy for each plot up to the layer where the maximum crown width per plot was obtained and took this height as separation plane for the upper and lower crown of the entire canopy. The relevant 3D point cloud of the airborne and terrestrial LIDAR measurements was cut along this plane and the relevant calculations were performed on this reduced 3D-dataset. The parameter “length of the shade canopy” was determined in the same way, typically the shade canopy length was about 90% of the whole tree height.

4 Results

4.1 Comparison of LAI and plant area indices derived from four different methods (litter traps, PCA, airborne and terrestrial laser scanning)

4.1.1 LAI from litter traps and PCA (LAI_L and LAI_{PCA})

Direct LAI measurements based on leaf litter collections (LAI_L) have been performed on 5 plots per species, so that 10 LAI_L values could be calculated.

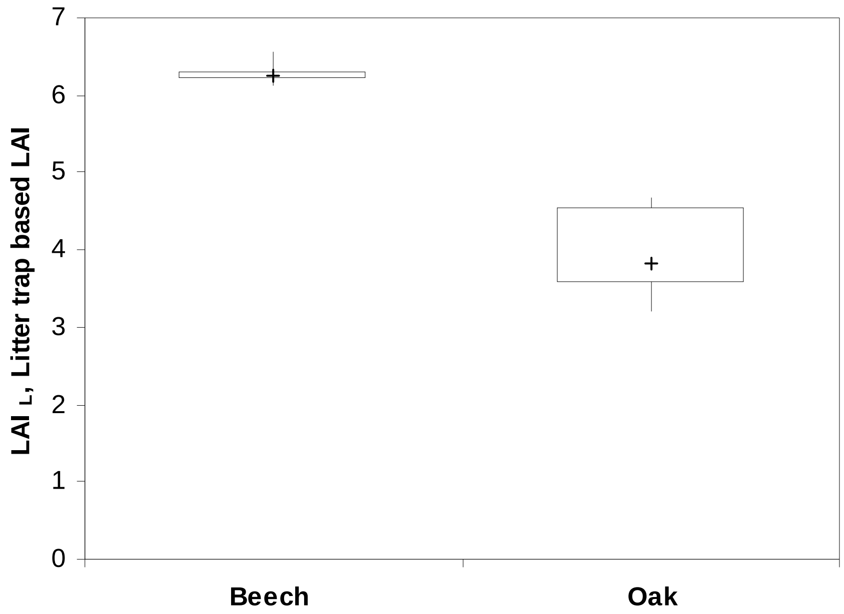

Fig. 2: The range of measured LAI-values for both species. Shown are minimum, maximum, median value and interquartile range.

The LAI_L-values of beech stands were all higher than those of oak stands and showed a remarkably low variability, with LAI_L ranging from 6.1 to 6.6. This can not be attributed to stand age, which varied from 60 to 145 years for beech and from 30 to 203 years for oak. Basal area (24-32m²/ha) was higher in the beech stands than in the oak stands (20-26m²), but still much more variable than LAI_L.

While the absolute values of LAI_L were lower in oak stands than in beech stands, their variability was higher. The highest value was 4.7 and originates from a 41 years old stand with comparably low stocks, while the oldest oak stands with the highest stocks reached medium LAI_L values (3.6, 4.1). The minimum value of 3.2 originates from an 82 years old oak stand with a basal area of 20 m².

PCA estimations should equal litter trap measurements in relative and absolute terms. The

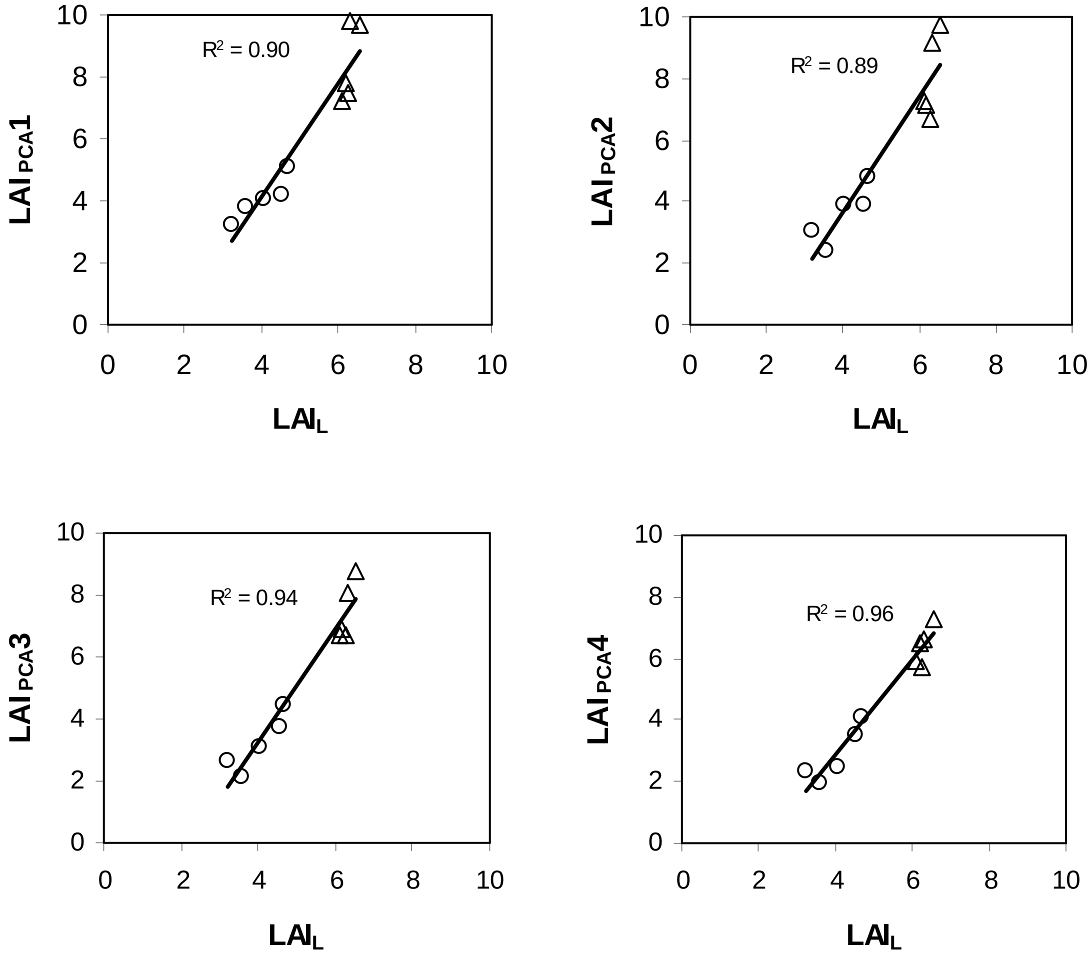

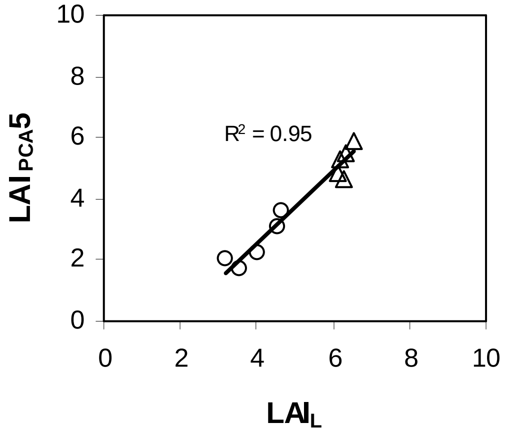

Fig. 3: Regressions between PCA-based LAI measurements and litter trap-based reference data. The PCA-based LAI has been calculated for 5 different opening angles including 1 up to 5 rings of the PCA-sensor. Oak stands are represented by open circles, Beech stands by open triangles.

comparison of LAI_{PCA} with LAI_L indeed shows a generally good correlation between both methods. Depending on the used opening angle of the instrument, regression coefficients ranged from 0.89 to 0.96 ($p<0.0001$). The relationship was best (0.94-0.96) for the higher opening angles, i.e., when rings 3, 4, or 5 of the PCA are included. In terms of absolute values, the root mean square error (RMSE) indicates the deviation of the 1:1 line and ranged from 0.9 to 1.7 in this case, indicating a certain degree of deviation between both methods (Fig. 4).

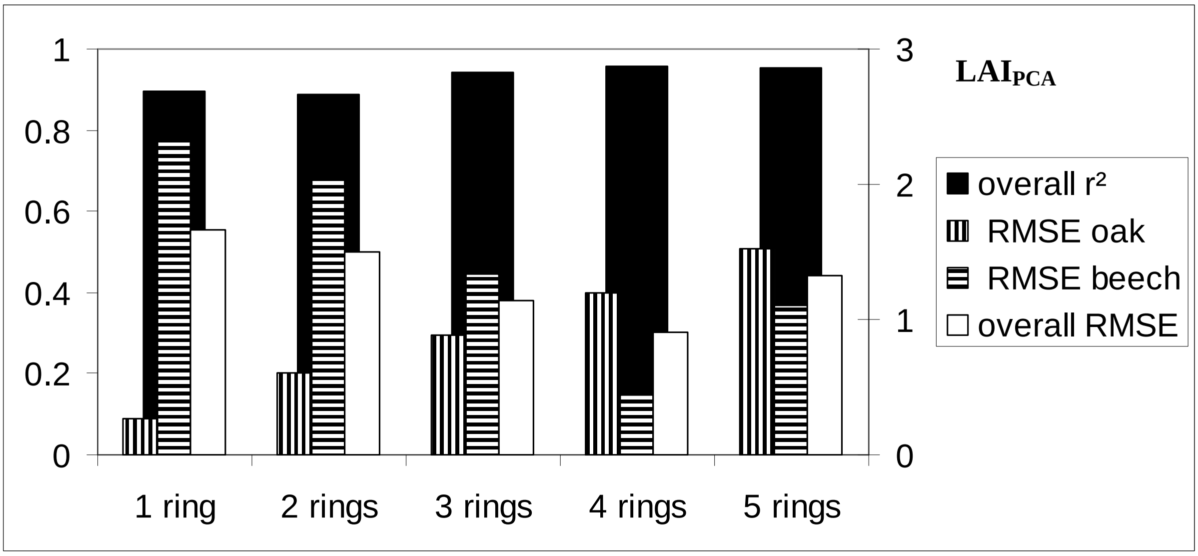

Fig. 4: Evaluation of LAI_{PCA} with LAI_L measurements. R^2 values for the whole dataset (black) are indicated on the left axis and RMSE-values for the whole dataset (white), for oak (vertically hatched), and for beech (horizontally hatched) are indicated on the right axis.

A species-specific analysis shows that RMSE for beech plots reached higher values (up to 2.3) than for oak plots (up to 1.5). The lowest absolute deviation (given as RMSE) between LAI_{PCA} and LAI_L values of the whole dataset is found, when 4 rings of the PCA are used (RMSE = 0.9). A tendency to underestimation on oak plots and overestimation on beech plots in these deviations is visible in the mean bias values (Fig. 5). The overall mean bias was lowest, when 3 rings of the PCA are used. Species-specific r^2-values were better for oak than for beech, but these data are questionable due to the low number of measurement points per species and the narrow range of values especially for beech.

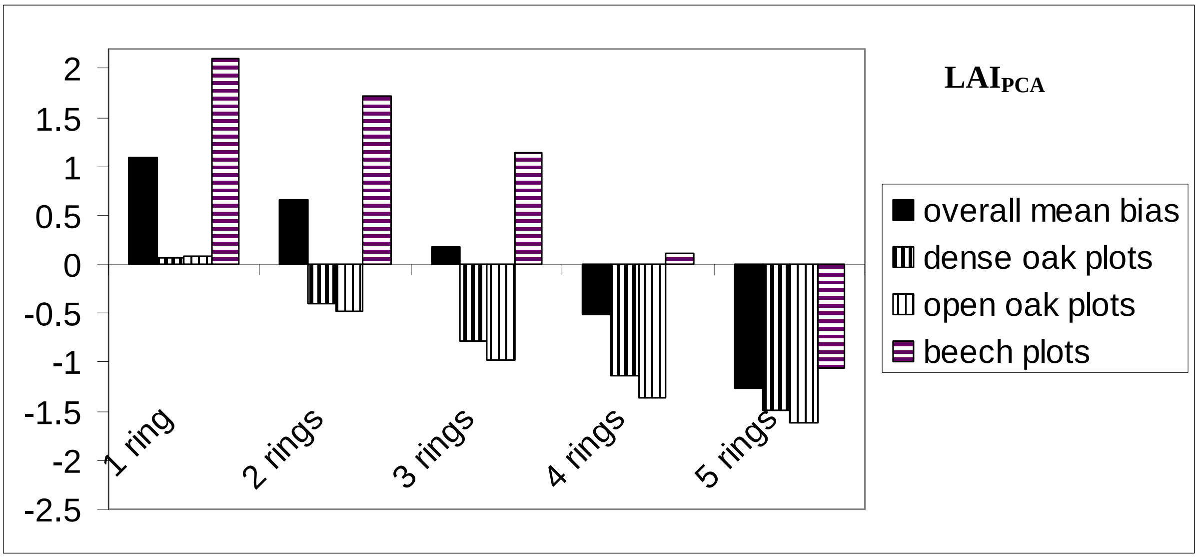

Fig. 5: Mean bias of LAI_{PCA} measurements when compared to LAI_L. Overall bias for all plots (black) is given and the separately calculated bias for 3 groups of plots: 2 dense oak plos (bold vertically hatched), 3 open oak plots (thin vertically hatched), and the 5 beech plots (horizontally hatched).

4.1.2 PCA-based gap fraction and plant area indices (GF_{PCA}, Le_{PCA}, Lt_{PCA})

The calculation of LAI_{PCA} includes intermediate results and plant area indices that are not yet corrected for the contribution of woody surfaces. These indices are analyzed here in order to better understand the causes for the relationship between LAI_{PCA} and LAI_L in the section before.

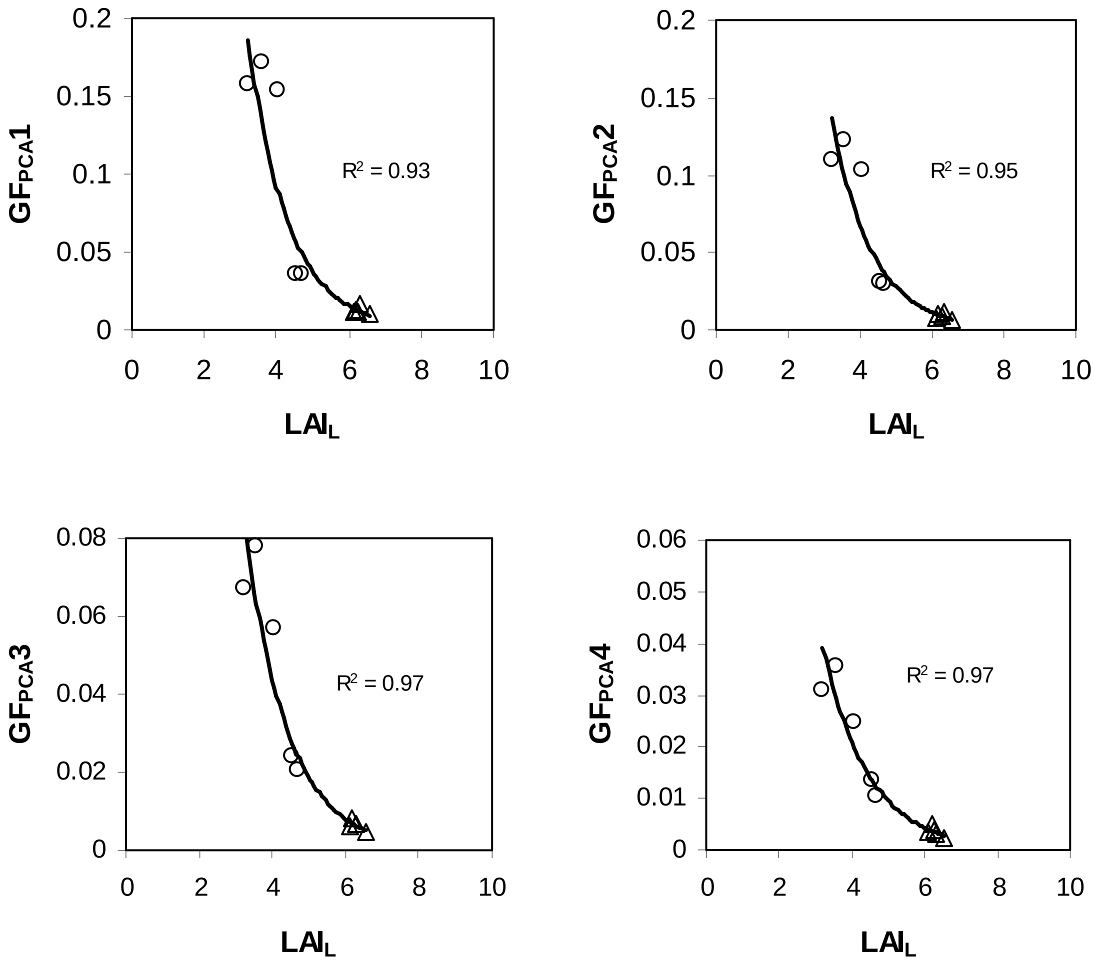

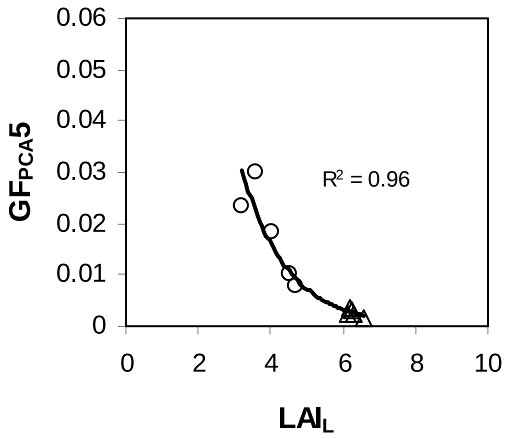

Fig. 6: Exponential dependence of PCA-based gap fraction (GF_{PCA}) on LAI_L. Oak stands are represented by open circles, beech stands by open triangles.

GF_{PCA}

GF_{PCA} is the gap fraction measured by the PCA sensor for each ring and is expected to be exponentially related to leaf area density in the canopy (equation 1). The corresponding graphs (Fig. 6) show that the non-linear coefficient of determination is even higher than in the linear correlations of Fig. 3. A separation of the data from 10 plots into 3 groups becomes visible: Unfortunately, all beech plots had nearly the same LAI_L- and gap fraction values and, thus, lie like one point on one end of the scale. Two denser oak plots lie very close together with intermediate LAI_L and gap fractions and the other 3 ("open") oak plots represent the lowest LAI_L values with the highest gap fractions. This arrangement in three groups is best visible in the one-ring and two-ring results and may have contributed to the high r^2-values of the exponential fits, though $r^2$was highest in the relationship for 3 rings and 4 rings and not for one and 2 rings. The narrow range of LAI_L-values for the beech plots is a challenge for the PCA-assessments and evaluations, since small measurement errors can easily result in a change of the ranking order of the 5 stands that could lead to misinterpretations.

The very fine differences that need to be assessed with the PCA when forest stands have LAI-values above 6 is visible in the beech stands in the 4-ring and 5-ring graph of Fig. 6, where differences in gap fraction (measured as relative light transmission) of less than 1% may cause a difference in LAI of ±2. The sensitivity of the inner rings to a variation in gap fraction is much lower: 1% GF_{PCA} variation corresponds to a variation in LAI_L of ±0.3.

Le_{PCA}

PCA gap fractions are converted after equation (3) into Le_{PCA}, which is due to the logarithmic transformation expected to show some kind of linear relationship to LAI_L. However, clumping effects and the contribution of woody surfaces to the measurement are not considered in Le_{PCA}. It anyway correlates very well with LAI_L, especially in the inner rings of the PCA sensor (Fig. 7). The narrow range of LAI_L-values of the beech plots was apparently not a problem in the measurements in the inner rings, since the ranking order of the stands was more or less conserved in the 1-ring, 2-rings and 3-rings measurement. r^2 for beech alone was best for the innermost ring (r^2= 0.66) and decreased with increasing ring number. This result is probably a direct consequence of the higher measurement accuracy in the inner rings that was shown in the GF_{PCA} results.

The slightly better r^2-values compared to LAI_{PCA} , which are especially valid for the innermost rings, go along with lower deviations between Le_{PCA} and LAI_L (Fig. 8) than between LAI_{PCA} and LAI_L (Fig. 4).

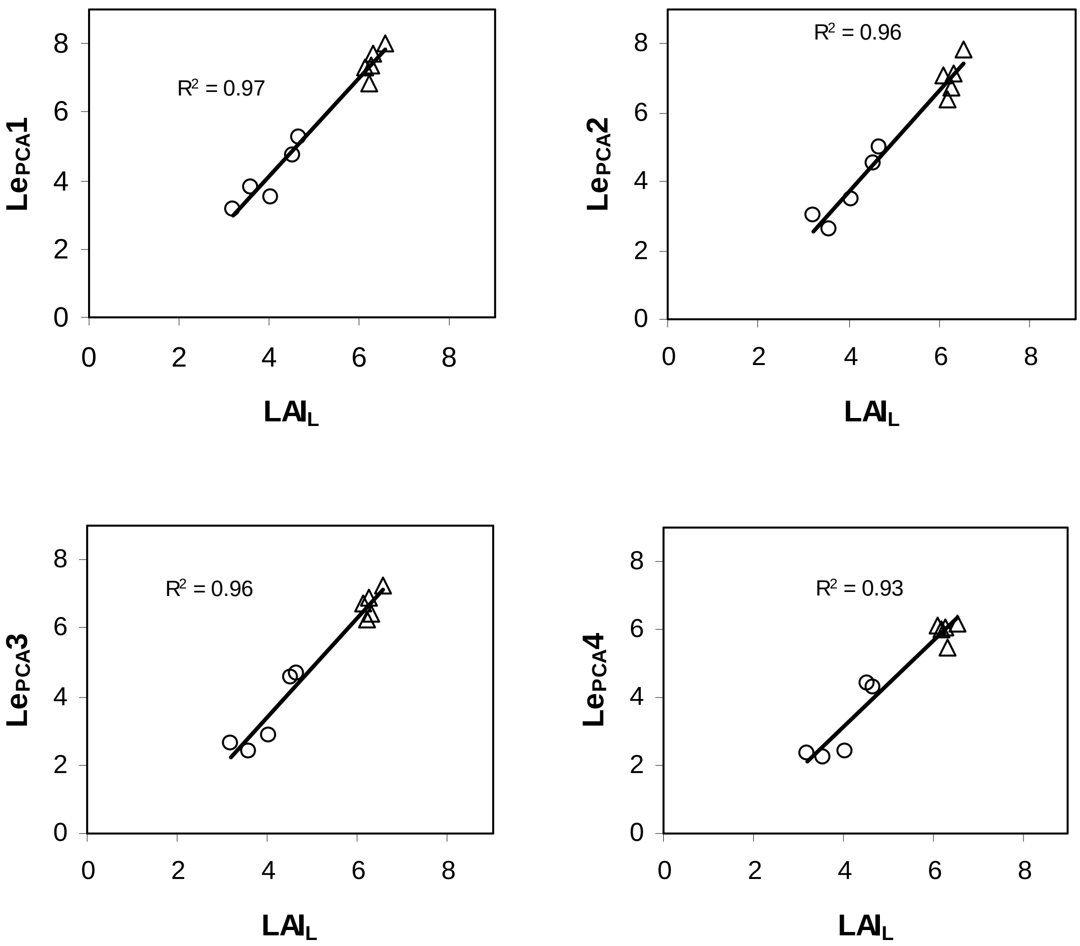

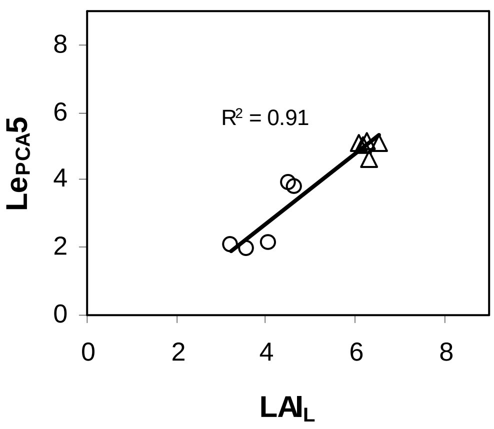

Fig. 7: Linear relationship of (Le_{PCA}) to $\mathrm{LAI_L}$. Oak stands are represented by open circles, beech stands by open triangles.

RMSE for the overall relationship ranged from 0.6 to 1.3, with the minimum RMSE occurring in the 3-ring $\mathrm{LAI_{PCA}}$. While oak stands had the lowest RMSE when only the innermost ring is evaluated, beech stands showed the minimum RMSE-deviation when 4 rings of the PCA sensor are used. Thus, r^2 and RMSE of $Le_{\mathrm{PCA}}5$ were worst, while the optimum combination of r^2 and RMSE was found in $Le_{\mathrm{PCA}}3$.

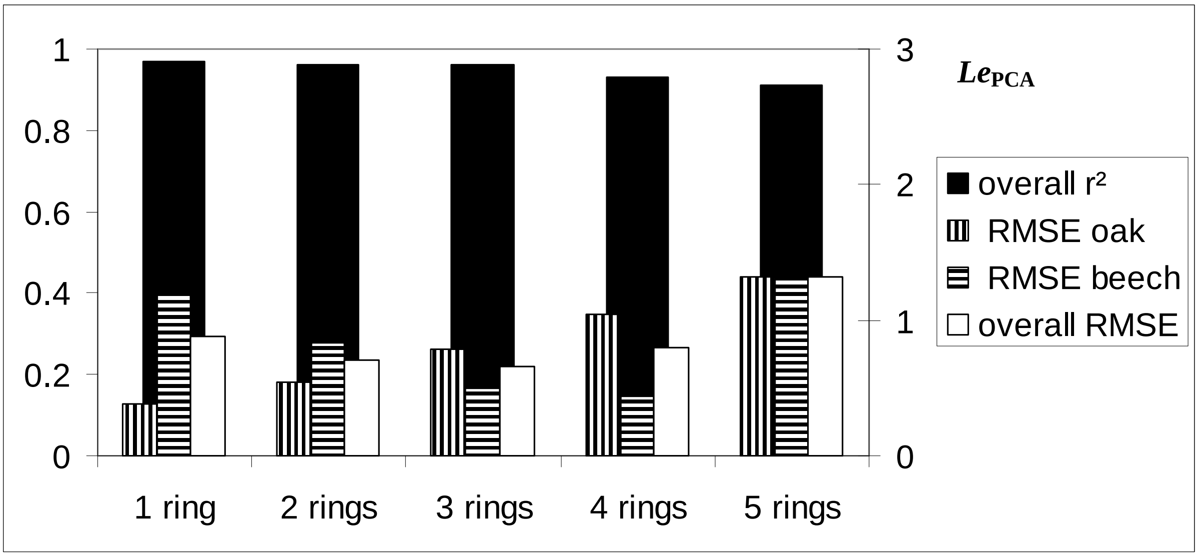

Fig. 8: R^2 and RMSE values for the relationship between Le_{PCA} and LAI_L. R^2 values for the whole dataset (black) are indicated on the left axis and RMSE-values for the whole dataset (white), for oak (vertically hatched), and for beech (horizontally hatched) are indicated on the right axis.

Apart from the effect of woody surfaces that causes an overestimation of LAI_L, Le_{PCA} does not include a correction for the clumped distribution of leaves in space that causes higher gap fractions than a random distribution and, thus, an underestimation of LAI_L. These expected under- or overestimations of LAI_L by Le_{PCA} were partly visible in the data (Fig. 9): LAI of all 3 groups of plots was underestimated in rings 4 and 5, so the effect of clumping must have had a stronger influence in these rings than the effect of woody surfaces. Generally the bias became more negative with increasing ring number. A possible explanation for this trend is that leaf inclinations in the investigated stands were mostly close to horizontal so that

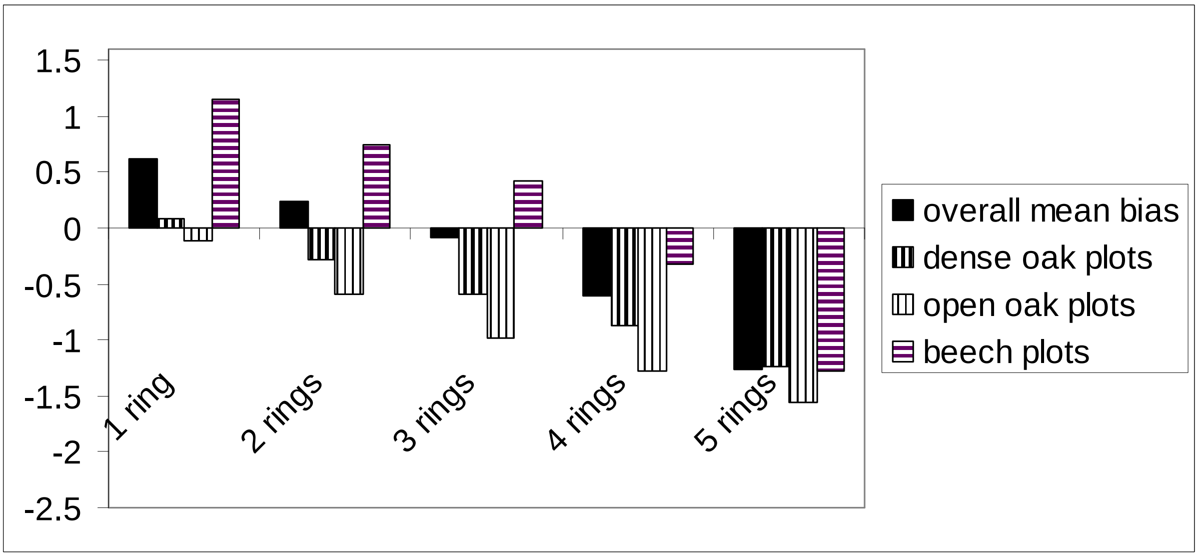

Fig. 9: Mean bias of Le_{PCA} measurements when compared to LAI_L. Overall bias for all plots (black) is given and the separately calculated bias for 3 groups of plots: 2 dense oak plos (bold vertically hatched), 3 open oak plots (thin vertically hatched), and the 5 beech plots (horizontally hatched).

clumping-induced gaps could more easily become effective in view angles that are close to horizontal. Overestimations did nearly not occur in oak stands but they occurred in the 3 innermost rings for beech. Apparently the contribution of woody surfaces to Le_{PCA} was more noticeable in stands with a very low gap fraction.

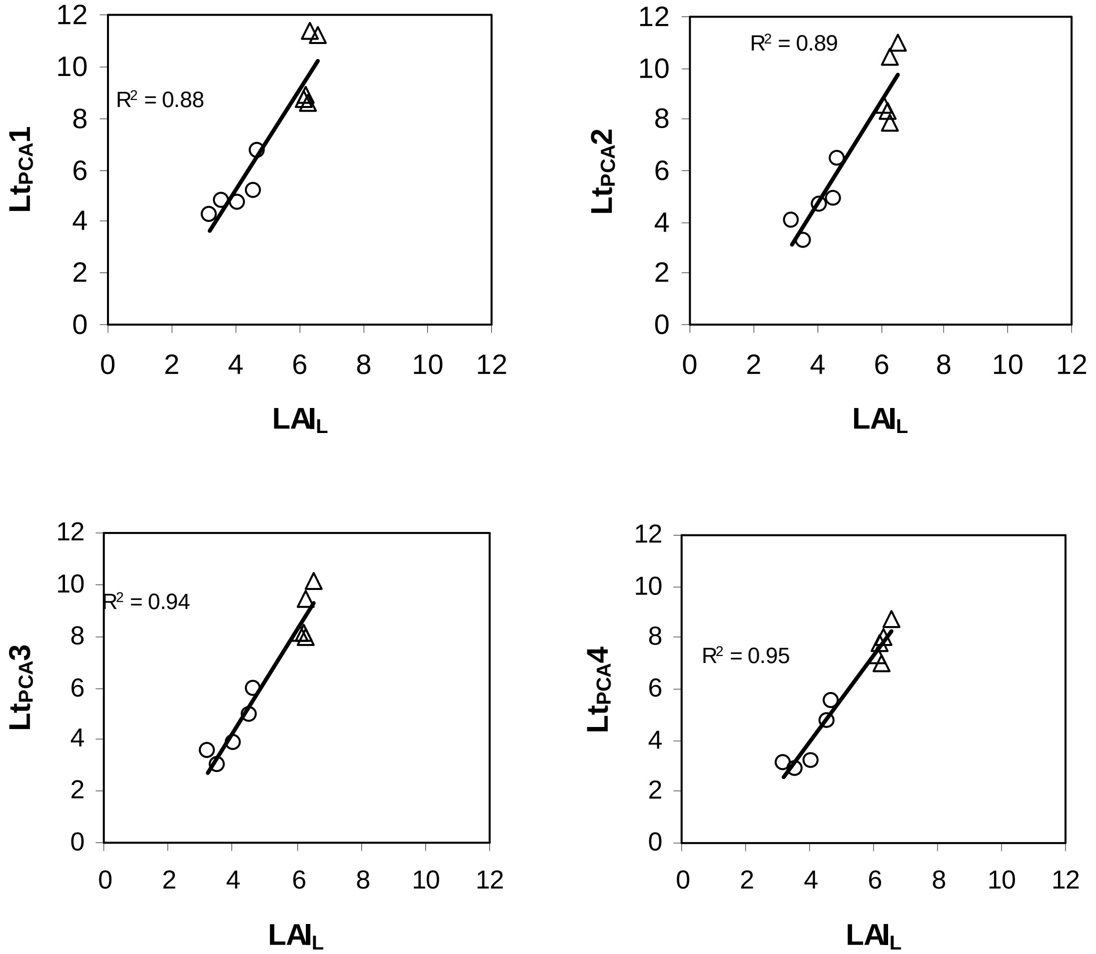

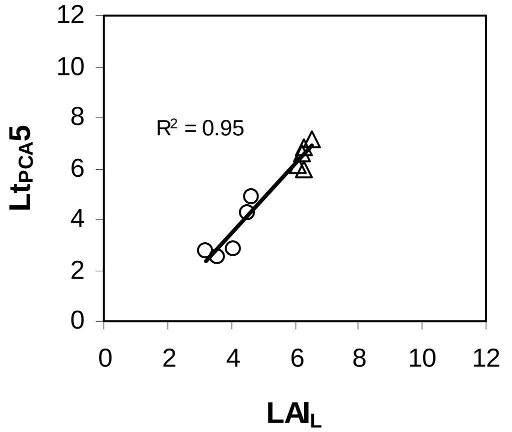

Fig. 10: Linear relationship of the total plant area index (Lt_{PCA}) to LAI_L. Oak stands are represented by open circles, beech stands by open triangles.

Lt_{PCA}

The effect of clumping correction based on TRAC measurements is visible in the total plant area index (Lt_{PCA}) shown in Figs. 10 and 11. The clumping coefficient Ω in equation (5) shall counteract the underestimation of LAI that is caused by clumped leaf distributions and thereby increased gap fractions. The underestimation that occurred when 4 or 5 rings are considered was indeed compensated for by Ω, so that RMSE and r^2 improved especially for the largest opening angle. For the lower opening angles, Lt_{PCA}-values increased to much too high values. The measured gap size distribution has apparently been most appropriate for the outermost rings, though the TRAC measurements employed were measured at an average angle of 32° in the case of beech plots and 49° in the case of the oak plots, which corresponds to ring 3 (beech) and ring 4 (oak).

While RMSE deviations got worse compared to Le_{PCA} (Fig. 8) in all cases except for the highest opening angle, r^2 increased for the two largest opening angles (rings 4 and 5) and decreased in the other cases. The higher RMSE-values in Fig. 11 are due to overestimations of the beech plots' LAI.

The final transformation of Lt_{PCA} to LAI_{PCA} has the objective to counteract the known overestimation, which is caused by the contribution of woody surfaces to the measured gap fraction. The effect was indeed a lower RMSE for the first 4 rings, only the highest opening angle had a higher RMSE after this transformation (compare Fig. 4).

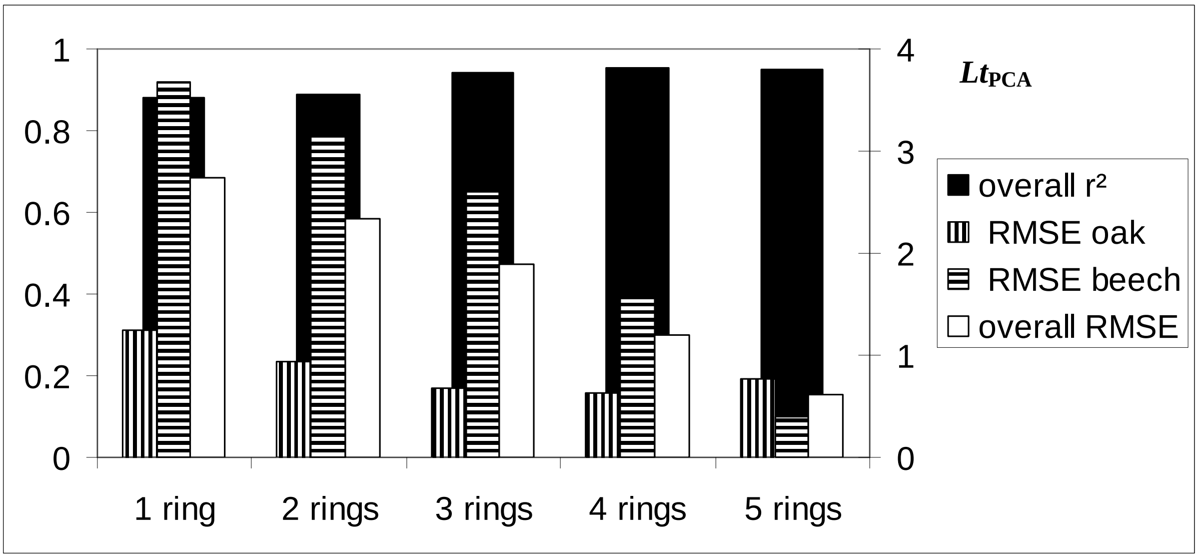

Fig. 11: R^2 and RMSE values for the relationship between Lt_{PCA} and LAI_L. R^2 values for the whole dataset (black) are indicated on the left axis and RMSE-values for the whole dataset (white), for oak (vertically hatched), and for beech (horizontally hatched) are indicated on the right axis.

4.1.3 ALS-based plant area index (L_{ALS})

Including the unweighted L_{ALS} after equation (7), four independently calculated forms of the airborne laser scanning derived plant area index are compared with the results of other measurement methods. The direct comparison with LAI_L values is possible based on the correlations to data from 10 plots (Fig. 12).

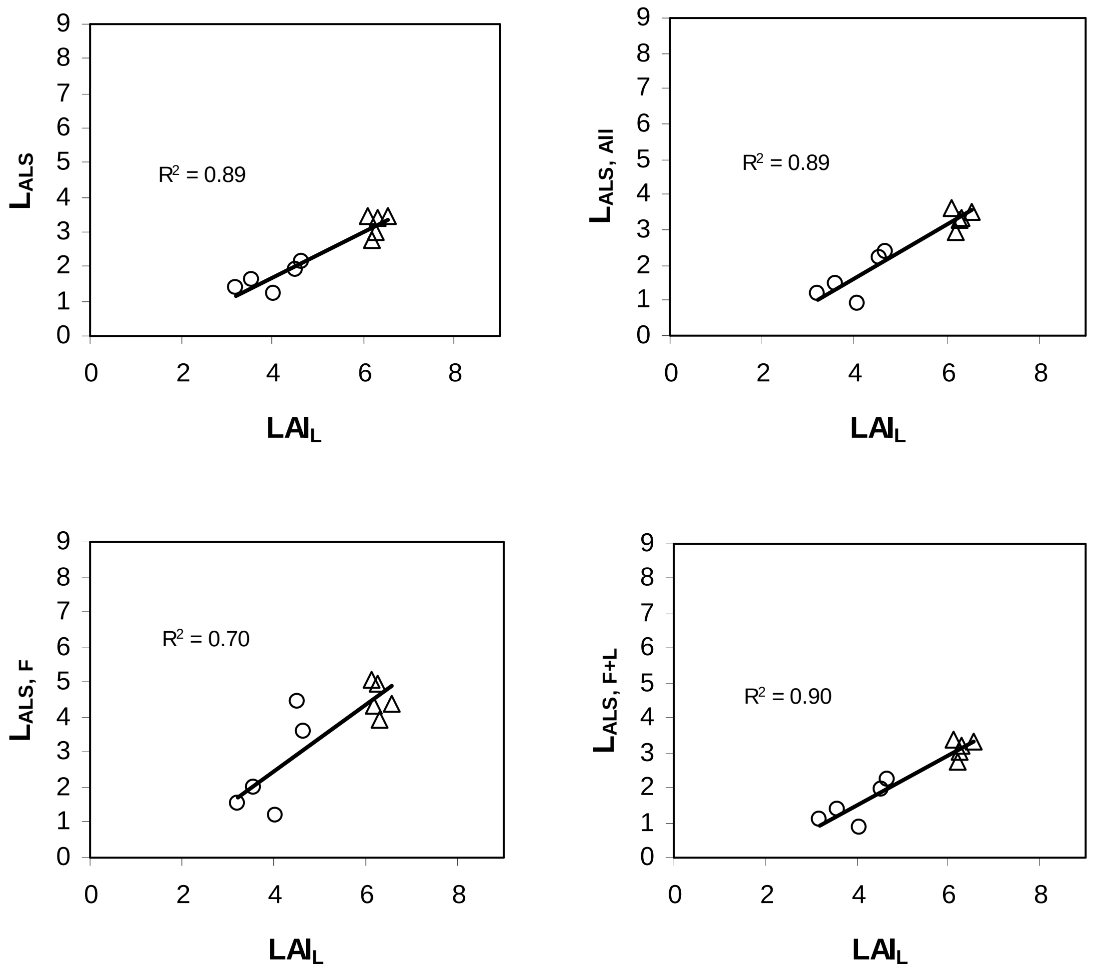

Fig. 12: Correlation of L_{ALS} , L_{ALS}All, L_{ALS}F, and L_{ALS}F+L to LAI_L. Oak stands are represented by open circles, beech stands by open triangles.

The highest r^2-value to LAI_L was achieved, when only first and last echoes were considered (L_{ALS}F+L, r^2=0.9), but also the weighted (L_{ALS}All, r^2=0.89) and unweighted (L_{ALS}, r^2=0.89) consideration of all echoes correlated very well with LAI_L. The consideration of only the first echoes was apparently less appropriate (L_{ALS}F, r^2=0.7).

A higher number of data points is available when LAI was determined with the PCA. This kind of LAI assessment was highly correlated to LAI_L with r^2 values up to 0.96 (LAI_{PCA}4, Fig. 3). A comparison of the four ALS-based plant area indices with LAI_{PCA}4 confirms the good results found in Fig. 12 (Fig. 13), but here L_{ALS} is best correlated, while L_{ALS}F has the lowest r^2 value and L_{ALS}All and L_{ALS}F+L are nearly as well correlated to LAI_{PCA}4 as L_{ALS}.

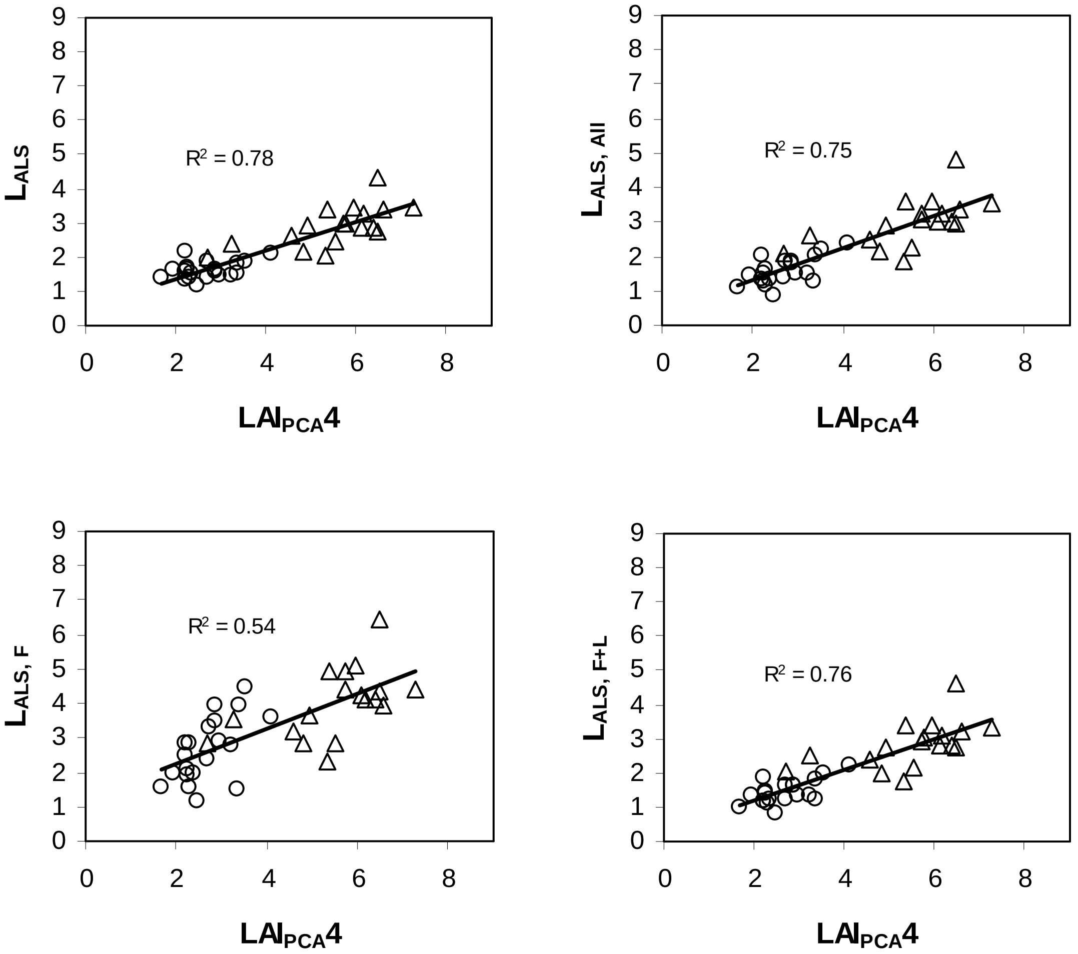

Fig. 13: Correlation of L_{ALS} , L_{ALS}All, L_{ALS}F, and L_{ALS}F+L to $LAI_{PCA}4$. Oak stands are represented by open circles, beech stands by open triangles.

This ranking order of r² values is exactly conserved for all opening angles of the PCA-sensor (Tab. 1) and the highest r² value is always achieved, when echoes are not weighted (L_{ALS}). The evaluation of 3 rings ($LAI_{PCA}3$) is mostly best correlated to the different ALS-derived plant area indices and is shown in Fig. 14.

L_{ALS} is a plant area index and, thus, not corrected for the contribution of woody surfaces to the measured quantity, so it should be better comparable with Le_{PCA} or Lt_{PCA} than with indirect or

R²	$LAI_{PCA}1$	$LAI_{PCA}2$	$LAI_{PCA}3$	$LAI_{PCA}4$	$LAI_{PCA}5$
L_{ALS}	0.80	0.81	**0.82**	0.78	0.72
L_{ALS}All	0.74	0.76	**0.77**	0.75	0.68
L_{ALS}F	0.45	0.49	0.52	**0.54**	0.50
L_{ALS}F+L	0.76	0.77	**0.78**	0.76	0.69

Tab. 1: r² values for ALS-derived plant area indices related to LAI-assessments with the PCA-sensor with different opening angles ($LAI_{PCA}1$ to $LAI_{PCA}5$)

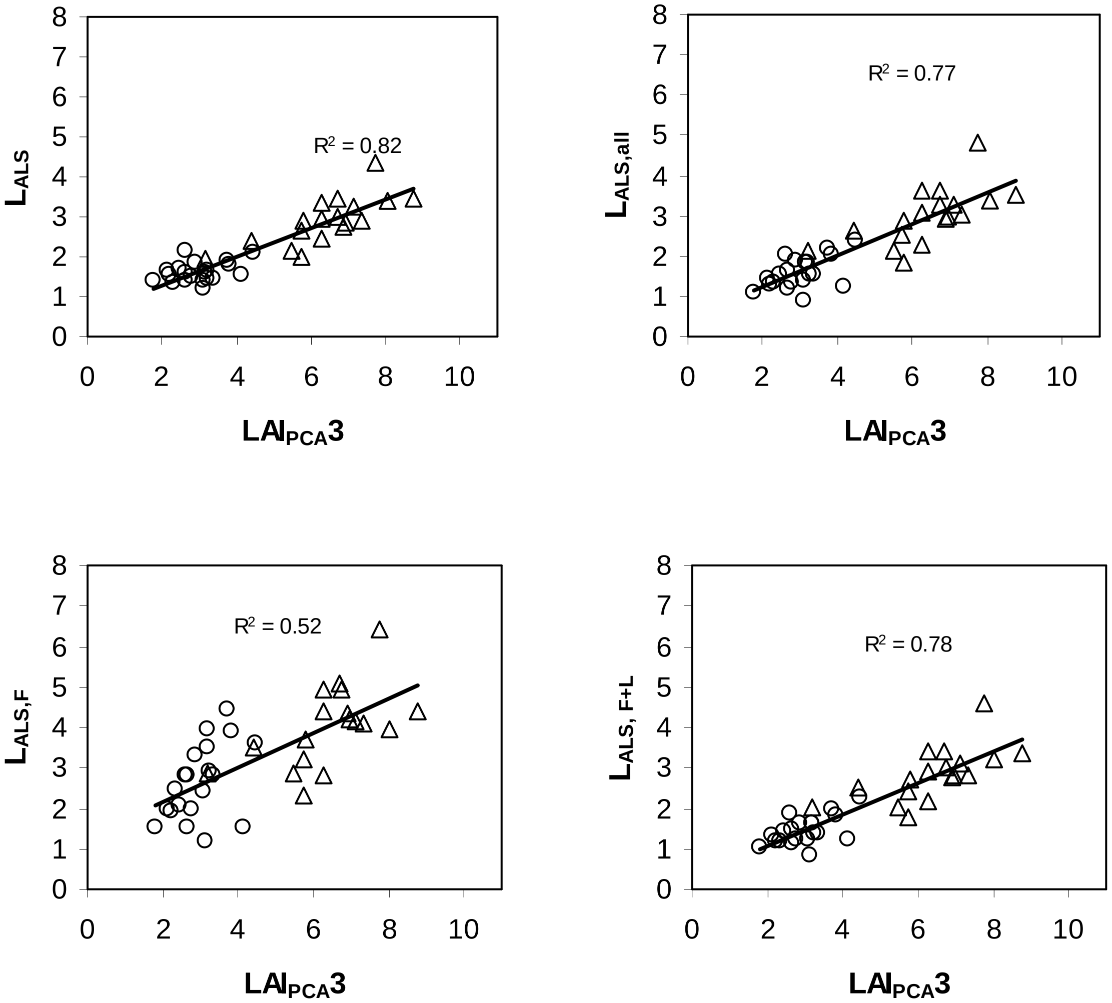

Fig. 14: Correlation of L_{ALS} , L_{ALS}All, L_{ALS}F, and L_{ALS}F+L to LAI_{PCA}3. Oak stands are represented by open circles, beech stands by open triangles.

direct LAI assessments. The r^2 values to the uncorrected PCA output (*Le*PCA) are indeed higher than to the derived LAI_{PCA} (Tab. 2). Best correlations (r^2=0.93) were found for L_{ALS}All and L_{ALS}F+L. The pattern of the best correlated PCA opening angle is similar to that of Tab. 1, with $Le_{PCA}3$ as mostly best correlated index (compare Fig. 15).

R^2	$Le_{PCA}1$	$Le_{PCA}2$	$Le_{PCA}3$	$Le_{PCA}4$	$Le_{PCA}5$
L_{ALS}	0.89	**0.91**	0.91	0.88	0.85
L_{ALS}All	0.89	0.92	**0.93**	0.92	0.90
L_{ALS}F	0.66	0.73	0.78	0.81	**0.83**
L_{ALS}F+L	0.90	0.93	**0.93**	0.92	0.89

Tab. 2: r^2 values for ALS-derived plant area indices related to effective leaf area index (Le_{PCA}) with different opening angles of the PCA sensor ($Le_{PCA}1$ to $Le_{PCA}5$)

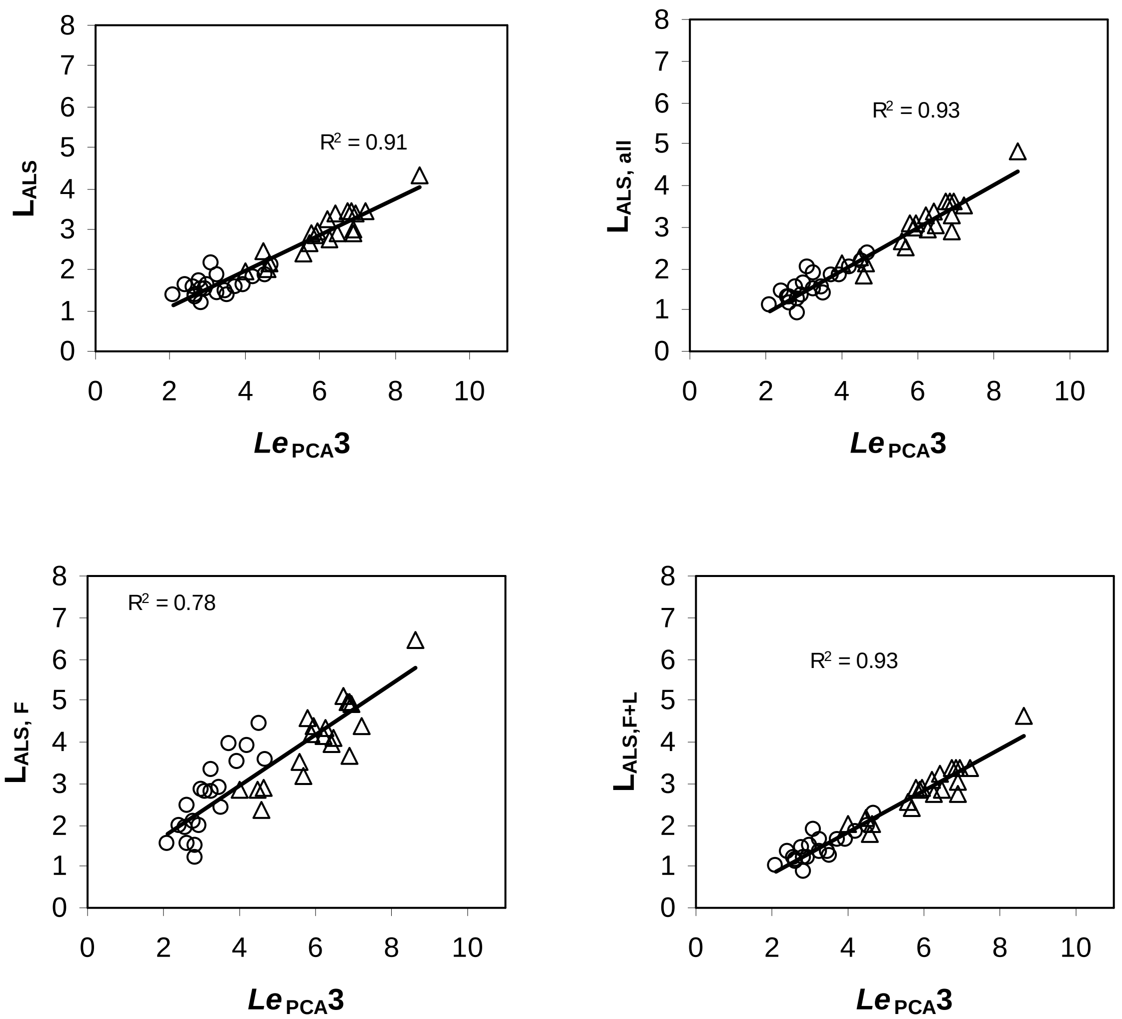

Fig. 15: Correlation of L_{ALS} , L_{ALS}All, L_{ALS}F, and L_{ALS}F+L to Le_{PCA}3. Oak stands are represented by open circles, beech stands by open triangles.

The clumping correction of Le_{PCA} leads to Lt_{PCA}, the total plant area index. This quantity is a bit weaker correlated to the ALS-derived plant area indices than LePCA, but r² values are still higher than for LAI_{PCA}, which is corrected for the contribution of woody surfaces (Tab. 3). Lt_{PCA} with an opening angle including ring 3 of the PCA-sensor is mostly best correlated to the ALS-derived plant area indices (Fig. 16).

R²	Lt_{PCA}1	Lt_{PCA}2	Lt_{PCA}3	Lt_{PCA}4	Lt_{PCA}5
L_{ALS}	0.84	0.84	**0.84**	0.81	0.78
L_{ALS}All	0.77	0.79	**0.80**	0.79	0.76
L_{ALS}F	0.48	0.53	0.57	**0.59**	0.59
L_{ALS}F+L	0.80	0.81	**0.82**	0.80	0.77

Tab. 3: r² values for ALS-derived plant area indices related to clumping corrected plant area indices of the PCA representing different opening angles (Lt_{PCA}1 to Lt_{PCA}5)

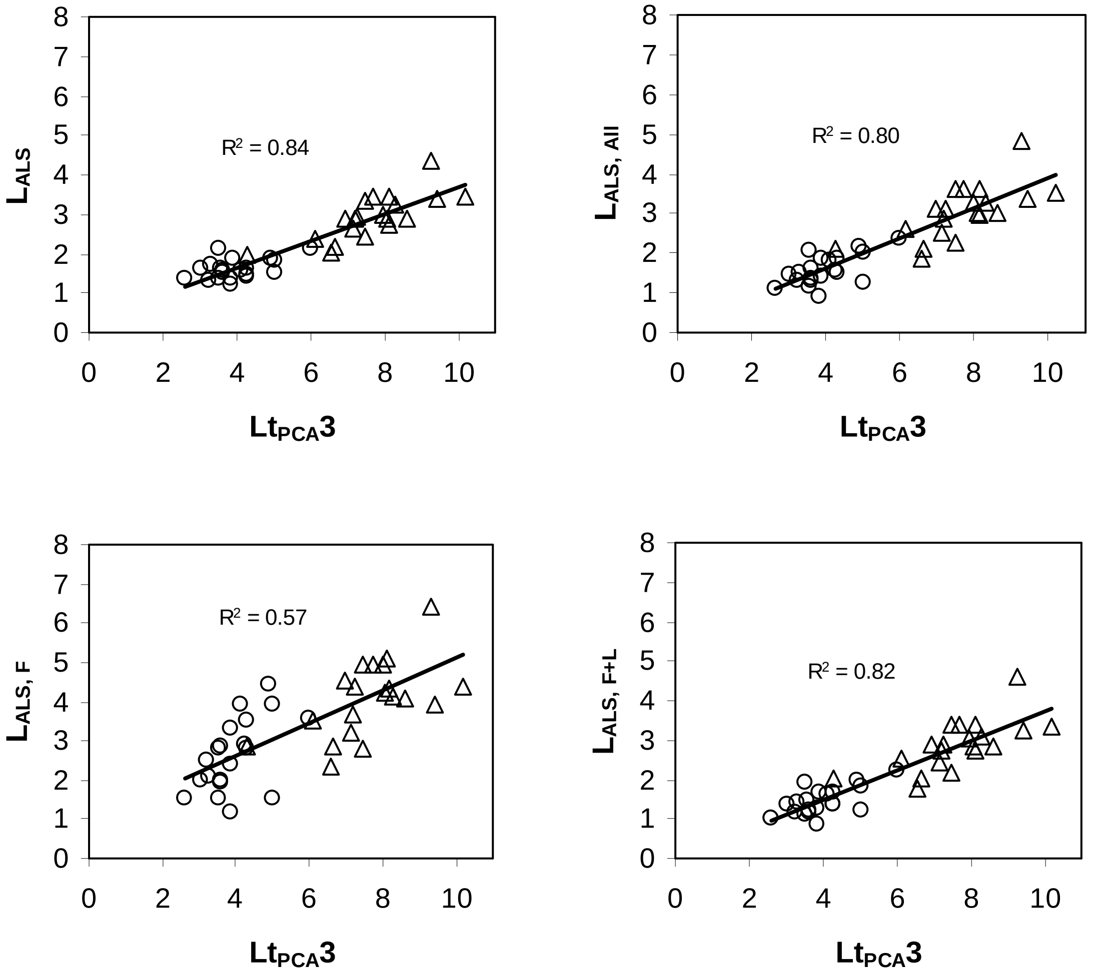

Fig. 16: Correlation of L_{ALS} , L_{ALS}All, L_{ALS}F, and L_{ALS}F+L to Lte_{PCA}3. Oak stands are represented by open circles, beech stands by open triangles.

Summarizing this section, all ALS-derived plant area indices except L_{ALS}F correlated with high r² values of about 0.9 to direct LAI-measurements (LAI$_L$, Fig. 12). Only the r² values to the raw instrument output of the PCA-sensor (effective leaf area index, Le_{PCA}, Fig. 15) were higher for L_{ALS}, L_{ALS}All and L_{ALS}F+L(up to r²=0.93). The clumping correction and the correction for woody surfaces decreased the coefficient of determination for these three indices to values between 0.77 and 0.84, if an opening angle corresponding to 3 rings of the PCA-sensor is used. This opening angle was in most cases best correlated to the ALS-derived plant area indices.

4.1.4 TLS-based plant area index (*L_{TLS}*)

The direct comparison between LAI_L and L_{TLS} shows that the suitability of the TLS-derived plant area index depends strongly on the resolution of the voxel model. The highest resolution used were voxels with an edge length of 10 cm (*L_{TLS}*10_2, *L_{TLS}*10_5, *L_{TLS}*10_7) and two of

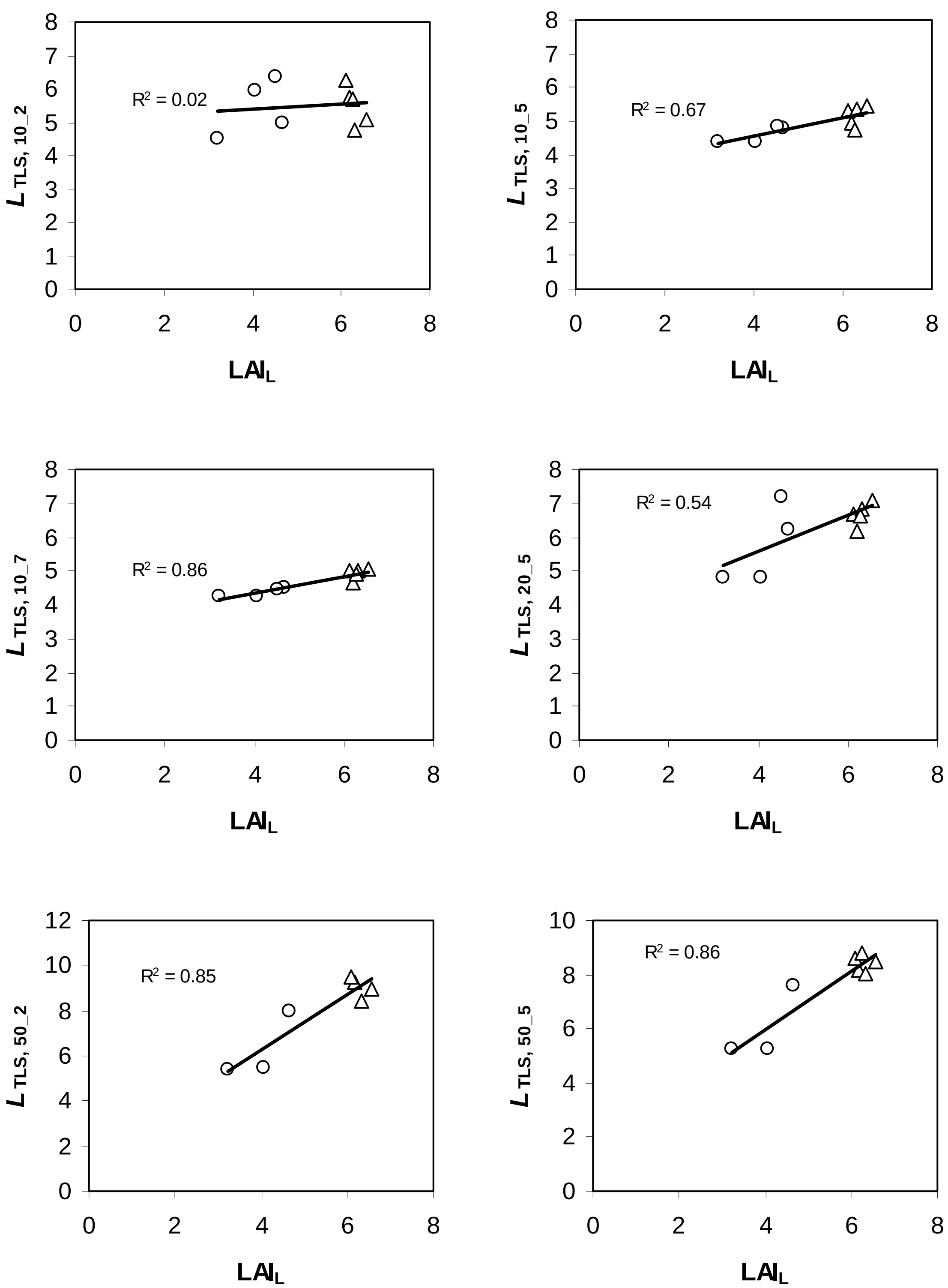

Fig. 17: Correlation of *L_{TLS}* in various resolutions to LAI_L. The resolution is given by two numbers in the variable name, from which the first number is voxel size in cm and the second number is the minimum number of points needed to create a voxel. Oak stands are represented by open circles, beech stands by open triangles.

these plant area indices were well correlated to LAI_L with r² values of 0.67 (L_{TLS}10_5) and 0.86 (L_{TLS}10_7). In the low resolution of 50cm voxel edge length, L_{TLS} for one plot could not be calculated due to 100% canopy cover in this resolution. With the same minimum point number of 5 points, the correlation was better for the higher resolution of 10cm (r^2=0.67) than for 20cm (r^2=0.54). A very low minimum point number was apparently disadvanatageous in a high resolution (L_{TLS}10_2: r² decreased to 0.02).

LAI_{PCA}

The low number of 9 data points (the TLS-data of one LAI_L-plot could not be evaluated) might on its own not be enough to draw conclusions from the LAI_L-data, but the available LAI_{PCA} data were so well correlated to LAI_L, that the same analysis can be executed on them. A number of 15 beech and 15 oak plots was available for this analysis. All opening angles of the PCA-sensor lead to good correlations between LAI_{PCA} and LAI_L (Fig. 3), and were, therefore, used for the comparison to L_{TLS} data, though LAI_{PCA}4 may be seen as most similar to LAI_L in this analysis.

R²	LAI_{PCA}1	LAI_{PCA}2	LAI_{PCA}3	LAI_{PCA}4	LAI_{PCA}5
L_{TLS}10_2	**0.01**	0.01	0.01	0.01	0.01
L_{TLS}10_5	0.71	**0.77**	0.76	0.75	0.74
L_{TLS}10_7	0.73	0.79	**0.79**	0.77	0.75
L_{TLS}20_5	0.48	0.54	0.56	**0.58**	0.57
L_{TLS}50_2	0.42	0.45	0.48	**0.51**	0.51
L_{TLS}50_5	0.45	0.50	0.53	**0.56**	0.55
L_{TLS}50_7	0.46	0.51	0.55	**0.57**	0.57

Tab. 4: r² values for TLS-derived plant area indices (different resolutions) related to PCA-derived LAI (LAI_{PCA}, different opening angles). The highest r² value in each row is highlighted.

The highest r² was found between L_{TLS}10_7 and LAI_{PCA}3 (r^2=0.79) and it is L_{TLS}10_7 that is always best correlated to LAI_{PCA} of the different opening angles. The ranking order of L_{TLS}10 and L_{TLS}20 values in terms of r² to any of the LAI_{PCA} is always the same as the one shown for LAI_L (Fig. 17), thus confirming these results. The higher r² for the L_{TLS}50 to LAI_L relationship is probably due to the lower plot number that could be evaluated. LAI_{PCA}4 was the opening angle that correlated best to most of the TLS-derived plant area indices, though it didn't reach the maximum r² value in this comparison.

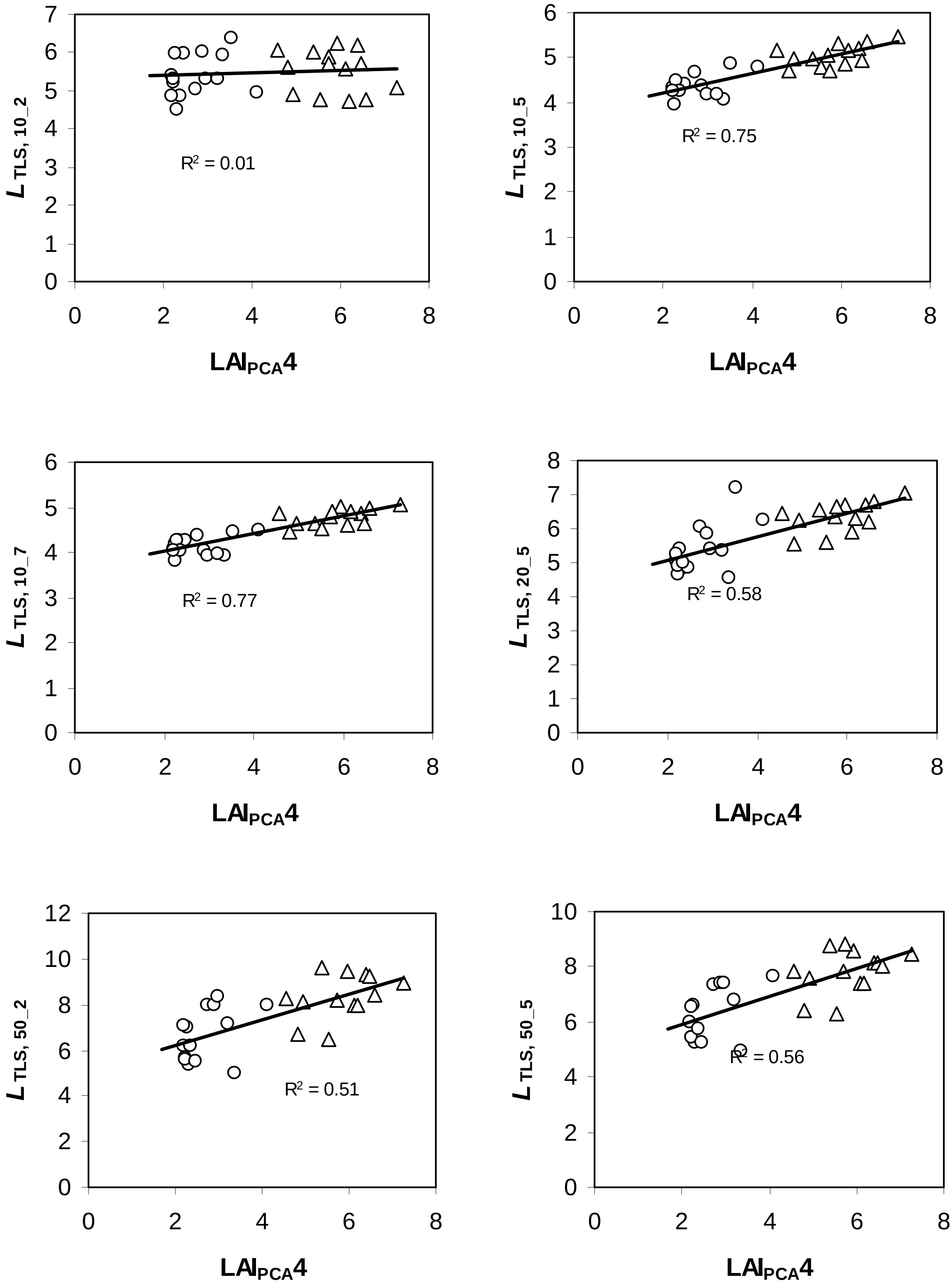

Fig. 18: Correlation of L_{TLS} in various resolutions to $\mathrm{LAI}_{\mathrm{PCA}}4$. The resolution is given by two numbers in the variable name, from which the first number is voxel size in cm and the second number is the minimum number of points needed to create a voxel. Oak stands are represented by open circles, beech stands by open triangles.

Le_{PCA}

Le_{PCA} and Lt_{PCA} are intermediate results in the determination of $\mathrm{LAI}_{\mathrm{PCA}}$ and, thus, closer to the original PCA-measurement. The uncorrected instrument output Le_{PCA} did even better correlate to LAI_L than the finally derived LAI_{PCA} values, with $Le_{PCA}3$ as the optimum value in terms or r², RMSE, and bias (Figs. 7-9). Also in comparison to L_{TLS}, Le_{PCA} correlated better than LAI_{PCA}(compare Tabs. 4 and 5), which is true for every single r² value. The highest r² value was found for the relationship between $L_{TLS}10\_7$ and $Le_{PCA}2$ (r^2=0.82), but $L_{TLS}10\_7$ was not always the best performing index: In comparison to the fifth ring, $L_{TLS}20\_5$ was better correlated than $L_{TLS}10\_7$ and so were the lower resolution values. Apart from the relationships to $Le_{PCA}5$ and to $L_{TLS}50$ values, the ranking order of r² values between $L_{TLS}10$ or $L_{TLS}20$ values and Le_{PCA} was for all other rings the same as for the relationship to LAI_L.

R²	$Le_{PCA}1$	$Le_{PCA}2$	$Le_{PCA}3$	$Le_{PCA}4$	$Le_{PCA}5$
$L_{TLS}10\_2$	0.03	0.04	0.04	**0.05**	0.05
$L_{TLS}10\_5$	0.75	**0.80**	0.79	0.76	0.75
$L_{TLS}10\_7$	0.77	**0.82**	0.81	0.77	0.75
$L_{TLS}20\_5$	0.64	0.70	0.74	0.76	**0.78**
$L_{TLS}50\_2$	0.59	0.64	0.69	0.74	**0.77**
$L_{TLS}50\_5$	0.63	0.69	0.75	0.78	**0.81**
$L_{TLS}50\_7$	0.63	0.70	0.75	0.77	**0.80**

Tab. 5: r² values for TLS-derived plant area indices (different resolutions) related to PCA-measured effective leaf area index (Le_{PCA}, different opening angles). The highest r² value in each row is highlighted.

The relationship of L_{TLS}-values, and especially of $L_{TLS}20\_5$, to the fifth ring of the PCA-sensor is more influenced by the amount of woody surfaces than any other quantity in this report (r^2=0.62), as may be seen from the Le_{PCA} measurements in the leafless stage in winter (Tab. 6).

R²	$Le_{PCA}1$winter	$Le_{PCA}2$winter	$Le_{PCA}3$winter	$Le_{PCA}4$winter	$Le_{PCA}5$winter
$L_{TLS}10\_2$	**0.04**	0.00	0.00	0.01	0.01
$L_{TLS}10\_5$	0.20	0.34	0.52	**0.56**	0.55
$L_{TLS}10\_7$	0.20	0.33	0.50	0.52	**0.55**
$L_{TLS}20\_5$	0.14	0.27	0.51	0.58	**0.62**
$L_{TLS}50\_2$	0.07	0.19	0.38	0.46	**0.50**
$L_{TLS}50\_5$	0.09	0.21	0.43	0.52	**0.58**
$L_{TLS}50\_7$	0.09	0.22	0.45	0.53	**0.59**

Tab. 6: r² values for TLS-derived plant area indices (different resolutions) related to PCA-measured effective leaf area index from the winter (Le_{PCA}winter, different opening angles). The highest r² value in each row is highlighted.

The increasing contribution of woody surfaces with increasing ring number of the *Le*PCA measurement may partly explain the tendency towards increasing r² values with increasing ring number shown for $L_{TLS}20$ and $L_{TLS}50$ in Tab. 5.

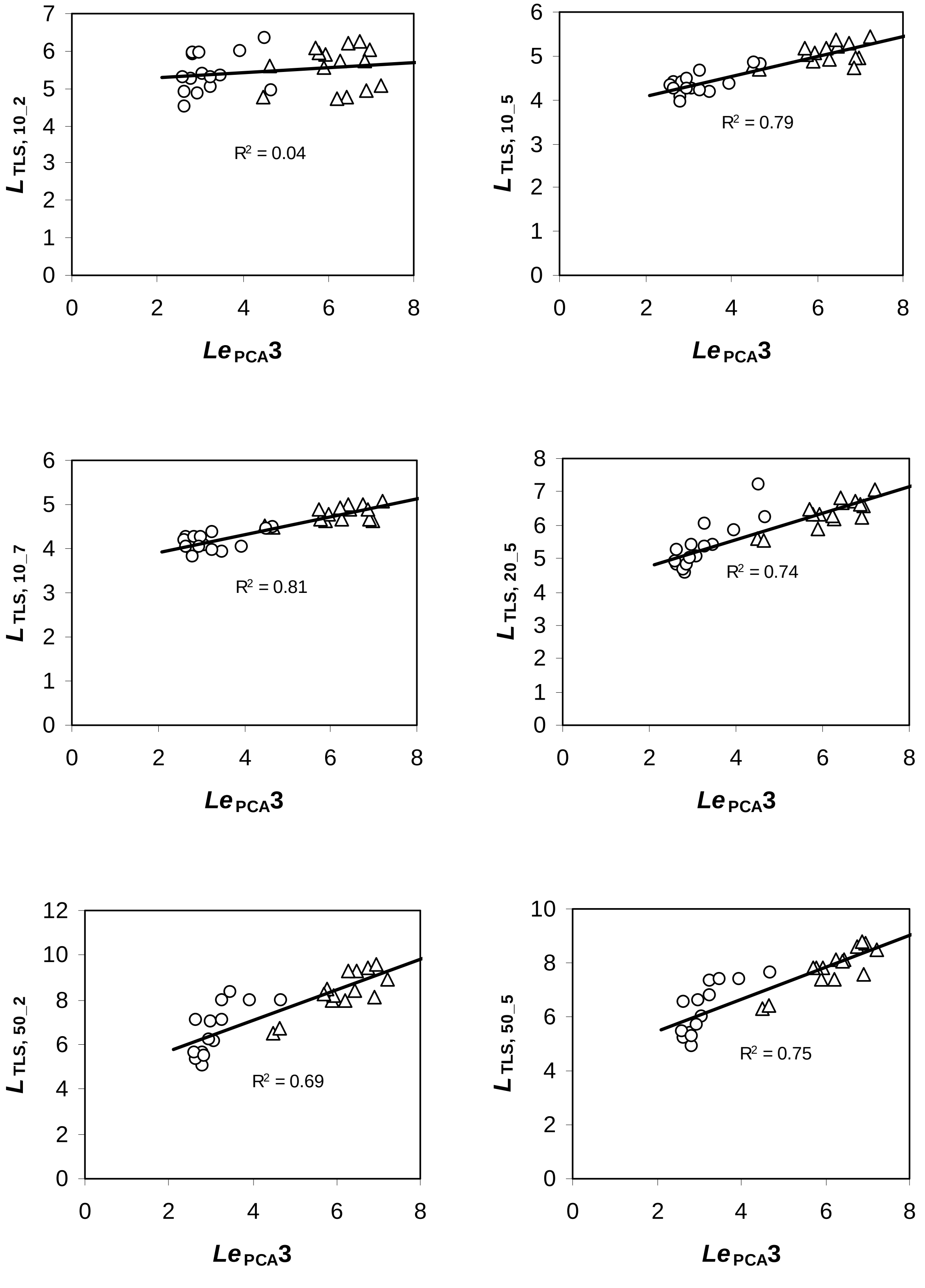

Fig. 19: Correlation of L_{TLS} in various resolutions to $Le_{PCA}3$. The resolution is given by two numbers in the variable name, from which the first number is voxel size in cm and the second number is the minimum number of points needed to create a voxel. Oak stands are represented by open circles, beech stands by open triangles.

The correlations of the TLS derived plant area indices to $Le_{PCA}3$, which was the opening angle most similar to LAI_L, are shown in Fig. 19.

Lt_{PCA}

The correlations of L_{TLS} indices with Lt_{PCA} , the clumping corrected PCA-derived plant area index, were very similar to those with Le_{PCA} (Tab. 7).

R²	$Lt_{PCA}1$	$Lt_{PCA}2$	$Lt_{PCA}3$	$Lt_{PCA}4$	$Lt_{PCA}5$
$L_{TLS}10\_2$	0.01	0.01	0.01	**0.01**	0.01
$L_{TLS}10\_5$	0.75	**0.79**	0.79	0.78	0.76
$L_{TLS}10\_7$	0.78	0.81	**0.81**	0.79	0.77
$L_{TLS}20\_5$	0.51	0.56	0.60	0.62	**0.62**
$L_{TLS}50\_2$	0.42	0.47	0.50	0.54	**0.54**
$L_{TLS}50\_5$	0.46	0.51	0.56	0.59	**0.59**
$L_{TLS}50\_7$	0.48	0.53	0.57	0.60	**0.61**

Tab. 7: r^2 values for TLS-derived plant area indices (different resolutions) related to PCA-measured plant area index (Lt_{PCA}, different opening angles). The highest r^2 value in each row is highlighted

L_{ALS}

When compared to the LAI measurements (LAI_L and LAI_{PCA}), the unweighted L_{ALS} was the most representative plant area index of the ALS derived indices and $L_{ALS}F$ was the least representative (compare Figs. 12 and 13 and Tab. 1). Anyway, for most of the L_{TLS} indices, the correlation was best to $L_{ALS}F$, indicating that the measured quantity of both methods describes something similar, which is not necessarily connected to LAI. Only the higher resolution L_{TLS} measurements ($L_{TLS}10\_5$ and $L_{TLS}10\_7$) correlated best to the unweighted L_{ALS} (Tab. 8).

R²	L_{ALS}	$L_{ALS}All$	$L_{ALS}F$	$L_{ALS}F{+}L$
$L_{TLS}10\_2$	0.01	0.03	**0.11**	0.03
$L_{TLS}10\_5$	**0.79**	0.78	0.59	0.78
$L_{TLS}10\_7$	**0.81**	0.78	0.57	0.79
$L_{TLS}20\_5$	0.63	0.73	**0.82**	0.71
$L_{TLS}50\_2$	0.57	0.69	**0.86**	0.66
$L_{TLS}50\_5$	0.63	0.76	**0.90**	0.73
$L_{TLS}50\_7$	0.65	0.76	**0.89**	0.73

Tab. 8: r^2 values for TLS-derived plant area indices (different resolutions) related to ALS-derived plant area index (L_{ALS}, different echo weightings). The highest r^2 value in each row is highlighted

In comparison the unweighted L_{ALS}, $L_{TLS}10\_7$ and $L_{TLS}10\_5$ performed best with r² values of 0.81 and 0.79, respectively (Fig. 20). The evaluation with respect to $L_{ALS}F$ yields partly r² values in a similar range, with $L_{TLS}50\_5$ as the best correlating index (r²=0.9, Fig. 21).

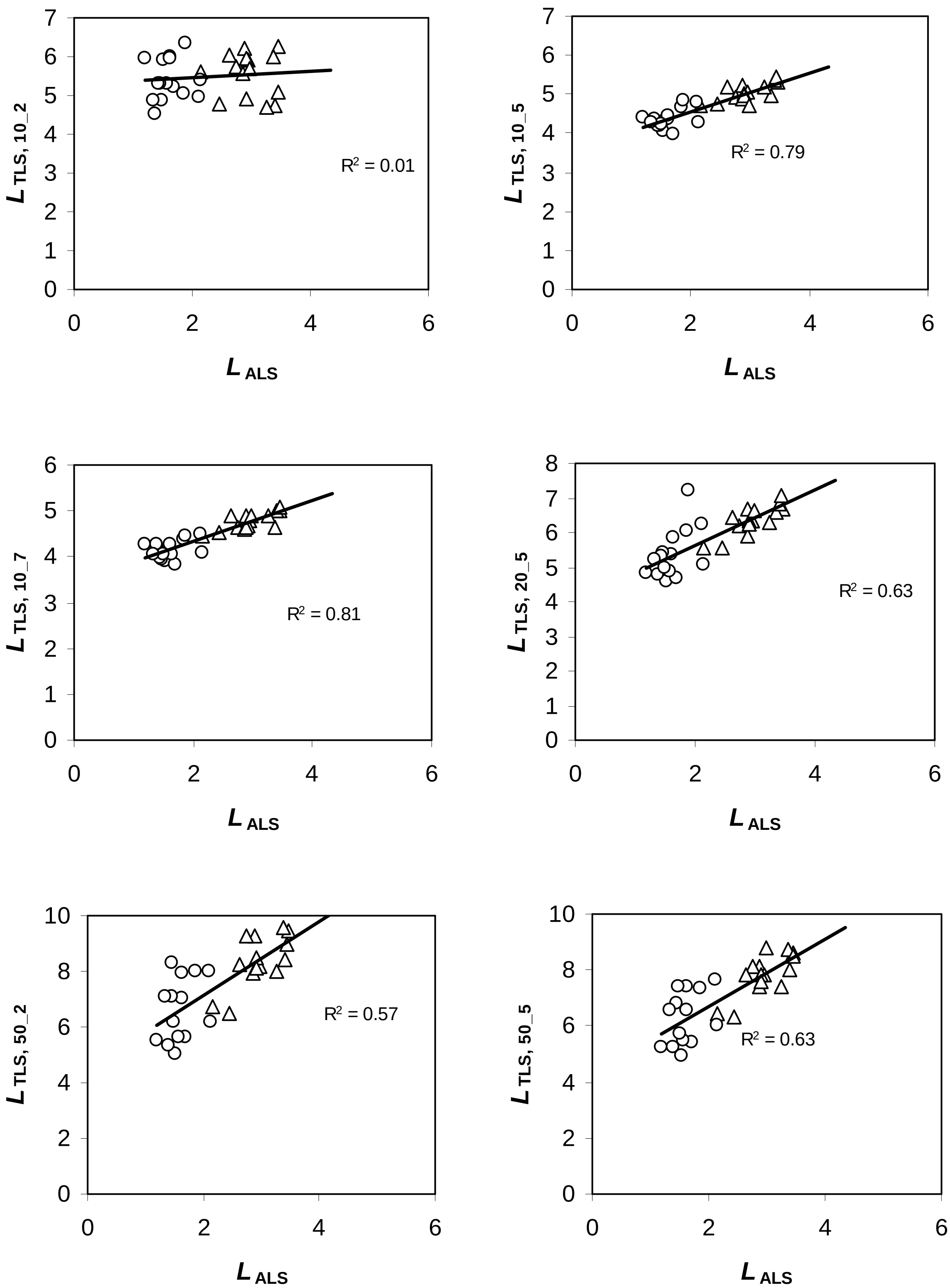

Fig. 20: Correlation of L_{TLS} in various resolutions to the unweighted L_{ALS}. The resolution is given by two numbers in the variable name, from which the first number is voxel size in cm and the second number is the minimum number of points needed to create a voxel. Oak stands are represented by open circles, beech stands by open triangles.

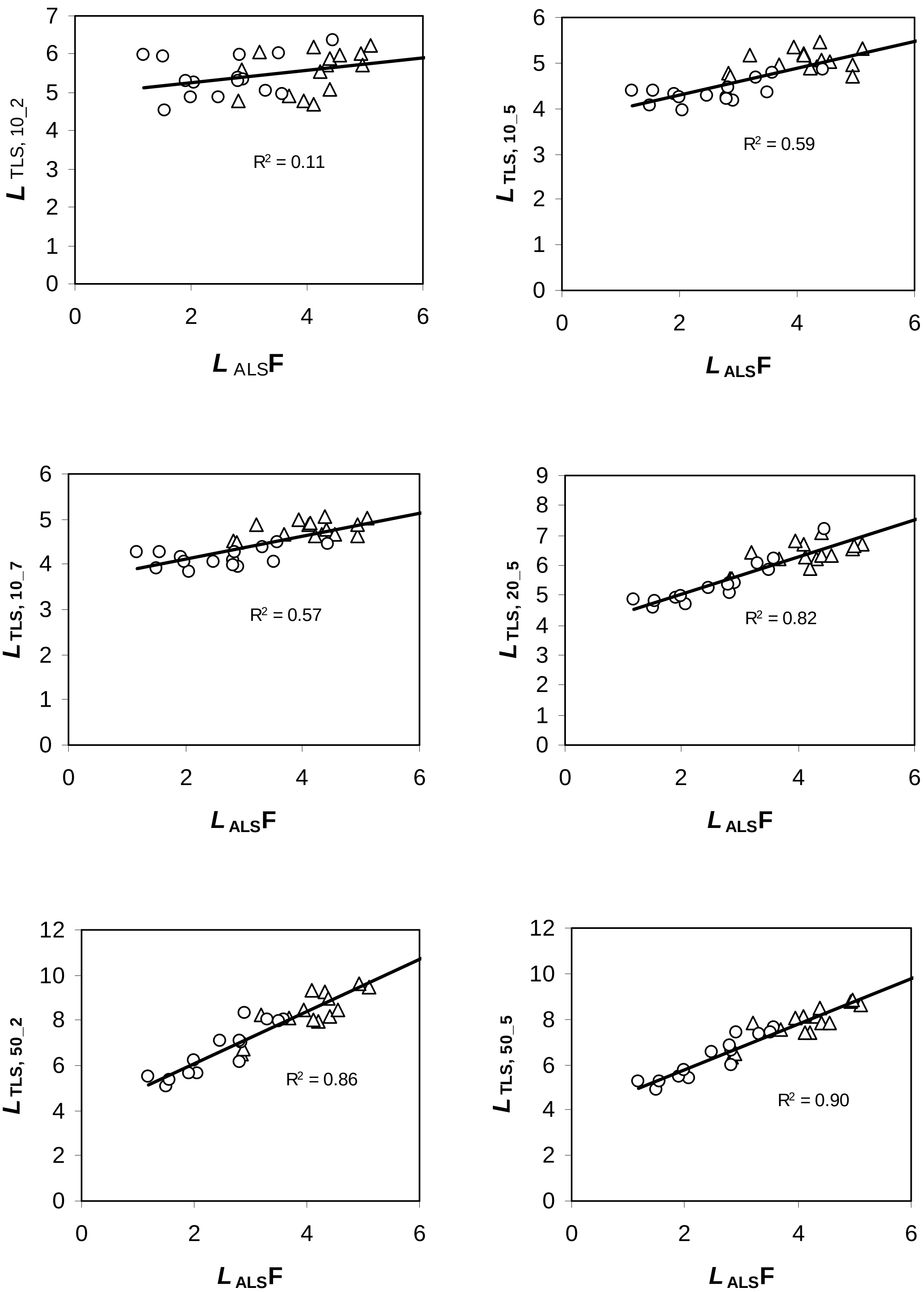

Fig. 21: Correlation of L_{TLS} in various resolutions to L_{ALS}F. The resolution is given by two numbers in the variable name, from which the first number is voxel size in cm and the second number is the minimum number of points needed to create a voxel. Oak stands are represented by open circles, beech stands by open triangles.

4.2 Relationship of crown condition measurements to different measures of LAI

The main difference between crown condition measurements and the several LAI measurements is their selective nature, i.e. that – in the case of ROLOFF, defoliation, and fruiting – only selected parts of the canopy are assessed in order to derive meaningful parameters. The leaf and plant area index measurement methods are not restricted to crown parts, but at least the airborne and terrestrial LIDAR measurements allowed a selective interpretation a posteriori by cutting the measured 3D-point cloud in a certain height.

4.2.1 Defoliation

From all basic stand parameters like age, basal area and tree height, defoliation was best correlated to age of the stand (r^2=0.41, Tab. 9 and Fig. 22). R^2-values to additional parameters like length of the shade canopy (p=0.08), leaf area index (LAI_L, p<0.01, r^2=0.23), and the clumping index that describes the clumped distribution of biomass in the canopy (p<0.01, r^2=0.18) were either not significant or lower than 0.25 (Tab. 9).

R^2 to…	Age of stand	Basal Area of stand	Height of trees	Length of shade canopy	Stocks of wood	LAI_L	Clumping Index
defoliation	**0.41**	n.s.	n.s.	n.s.	0.12	0.23	0.18

Tab. 9: r^2 values for defoliation related to basic stand attributes including LAI_L and clumping index. The highest r^2 value is highlighted, n.s. means not significant.

Relationship to PCA-measurements

All correlations between defoliation and PCA-derived leaf or plant area indices were significant with p<0.001, with a maximum r^2 value reached in the relationship to $GF_{PCA}5$

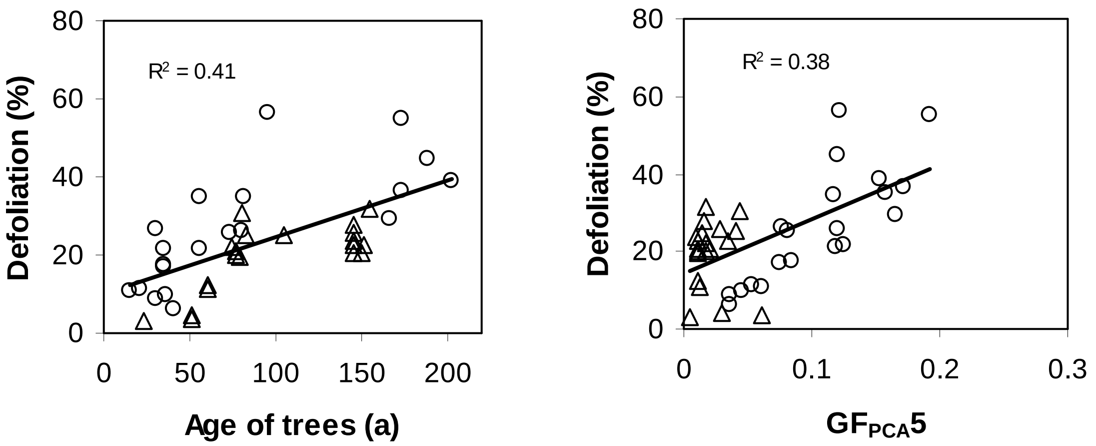

Fig. 22: Correlations of defoliation to age of trees and the gap fraction measurement of the PCA ($GF_{PCA}5$). Oak stands are represented by open circles, beech stands by open triangles.

(r^2=0.38, Tab. 10 and Fig. 22). The gap fraction is a type of light transmission measurement and, therefore, to some extent similar to the defoliation assessment.
The highest coefficients of determination were usually reached, when the whole information of all 5 rings was used for the calculation. The more the original gap fraction value is transformed by calculations and corrections, the lower was the achieved r^2. Le_{PCA} (r^2=0.27) and Le_{PCA},winter (r^2=0.29) were quite similarly related to defoliation. The finally derived LAI_{PCA} (r^2=0.1) was least correlated to defoliation and even less correlated than LAI_L.

R^2 to defoliation	Ring 1	Ring 2	Ring 3	Ring 4	Ring 5
GF_{PCA}	0.31	0.28	0.34	0.37	**0.38**
Le_{PCA}	0.14	0.19	0.22	0.24	**0.27**
Lt_{PCA}	0.06	0.09	0.11	0.13	**0.13**
LAI_{PCA}	0.07	0.09	0.10	**0.10**	0.09
$Le_{PCA,\ winter}$	0.00	0.04	0.17	0.23	**0.29**

Tab. 10: r^2 values for defoliation related to PCA-derived indices: GF_{PCA}, Le_{PCA}, Lt_{PCA}, LAI_{PCA}, and $Le_{PCA,winter}$. The highest r^2 value in each row is highlighted.

Relationship to ALS-measurements

All correlations between defoliation and ALS-derived gap fraction and plant area indices were significant with $p<0.001$ (Tab. 11). The differences between the different parts of the canopy (whole canopy, upper canopy, and lower canopy) were marginal and the results for the upper canopy were sometimes worse than those from the whole canopy. The upper canopy had an average height extension of 3.5m.
GF_{ALS}F (see Fig. 23) and L_{ALS}F, which is the ALS-derived plant area index with the weakest correlation to LAI_L, had always the highest r^2 value in relation to defoliation (r^2=0.41 and 0.36, respectively). Both quantities are derived only from the first echoes of the laser signal received from above the canopy.

R^2 to defoliation	unweighted	All	F	F+L
GF_{ALS}	0.11	0.28	**0.41**	0.26
$GF_{ALS,\ lower}$	0.09	0.21	**0.40**	0.24
$GF_{ALS,\ upper}$	0.15	0.25	**0.39**	0.28
L_{ALS}	0.09	0.19	**0.36**	0.18
$L_{ALS,\ lower}$	0.07	0.17	**0.36**	0.16
$L_{ALS,\ upper}$	0.12	0.18	**0.32**	0.17

Tab. 11: r^2 values for defoliation related to ALS-derived gap fractions and plant area indices (different echo weightings): GF_{ALS}, $GF_{ALS,\ lower}$, $GF_{ALS,\ upper}$, L_{ALS}, $L_{ALS,\ lower}$, and $L_{ALS,\ upper}$. The highest r^2 value in each row is highlighted.

Relationship to TLS-measurements

All correlations between defoliation and TLS-derived gap fraction and plant area indices were significant with $p<0.001$ (Tab. 12). Though the high resolution values derived from a voxel model with edge length of 10cm were best correlated to LAI_L, they didn't achieve high correlations to defoliation. Here the GF_{TLS} and L_{TLS} indices with the lower resolution of 20 or 50cm reached the highest r²-values (GF_{TLS}20_5, r^2 =0.44; L_{TLS}50_5, r^2=0.41; Fig. 23). The results for the separately calculated upper canopy (average height extension: 3.5m) were always worse than those for the whole canopy.

R² to defoliation	10_2	10_5	10_7	20_5	50_2	50_5	50_7
GF_{TLS}	0.11	0.33	0.32	**0.44**	0.37	0.39	0.39
$GF_{TLS, lower}$	0.10	0.31	0.30	**0.40**	0.35	0.37	0.37
$GF_{TLS, upper}$	0.00	0.06	0.06	0.07	**0.11**	0.08	0.08
L_{TLS}	0.08	0.07	0.04	0.30	0.39	**0.41**	0.39
$L_{TLS, lower}$	0.03	0.02	0.01	0.20	0.33	**0.34**	0.31
$L_{TLS, upper}$	0.03	0.04	0.04	0.06	**0.11**	0.09	0.09

Tab. 12: r² values for defoliation related to TLS-derived gap fractions and plant area indices (different voxel model resolutions): GF_{TLS}, $GF_{TLS, lower}$, $GF_{TLS, upper}$, L_{TLS}, $L_{TLS, lower}$, and $L_{TLS, upper}$. The highest r² value in each row is highlighted.

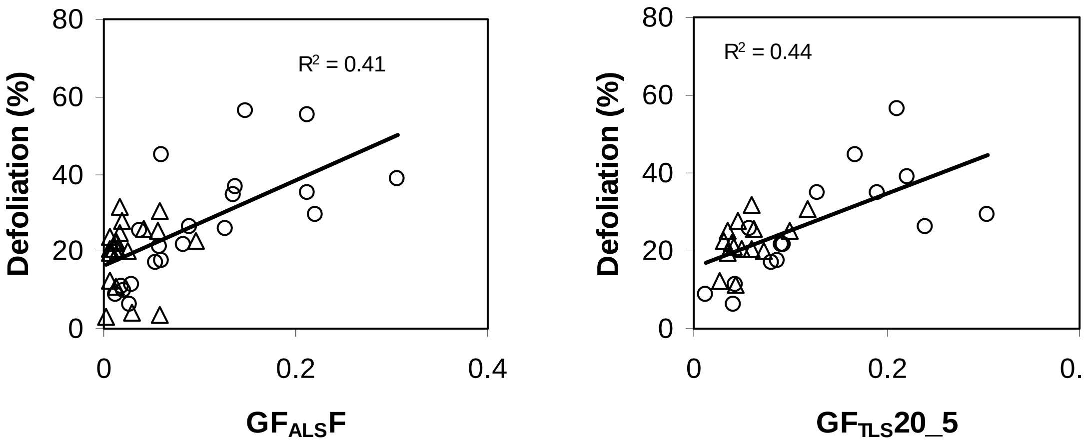

Fig. 23: Correlations of defoliation to ALS- and TLS-derived gap fraction measurements (GF_{ALS}F and GF_{TLS}20_5). Oak stands are represented by open circles, beech stands by open triangles.

4.2.2 Apical shoot architecture (ROLOFF)

All relationships between the ROLOFF assessment and basic stand parameters describing the physiological stage of the stand, the amount of biomass and its distribution were significant with $p<0.01$ (Tab. 13). The closest relationship was found between ROLOFF and stand age (Fig. 24). From the biomass parameters, length of the shade canopy was best correlated to ROLOFF, while basal area showed no clear relationship.

R^2 to…	Age of stand	Basal Area of stand	Height of trees	Length of shade canopy	Stocks of wood	LAI_L	Clumping Index
ROLOFF	**0.70**	0.05	0.39	0.41	0.37	0.16	0.11

Tab. 13: r^2 values for defoliation related to basic stand attributes including LAI_L and clumping index. The highest r^2 value is highlighted.

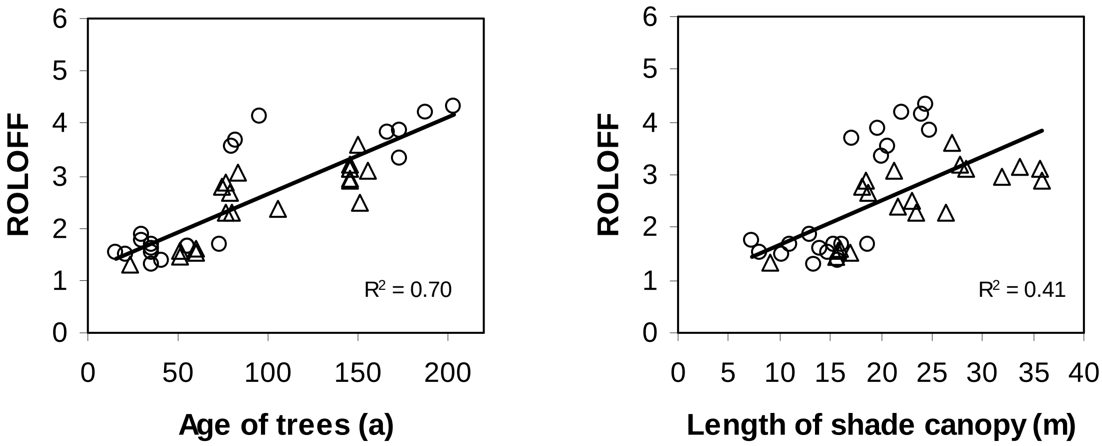

Fig. 24: Correlations of apical shoot architecture (ROLOFF) to stand age and length of the shade canopy. Oak stands are represented by open circles, beech stands by open triangles.

Relationship to PCA-measurements

While all relationships between ROLOFF and any of the PCA-measured quantities were significant, none of them reached an r^2 value higher than 0.13 (GF_{PCA}, Tab. 14). The Le_{PCA} winter measurements (without leaves, r^2=0.1) were better correlated than the summer measurements (r^2=0.04).

R^2 to ROLOFF	Ring 1	Ring 2	Ring 3	Ring 4	Ring 5
GF_{PCA}	0.03	0.02	0.06	0.09	**0.13**
Le_{PCA}	0.00	0.00	0.02	0.03	**0.04**
Lt_{PCA}	0.00	0.00	0.00	0.00	**0.01**
LAI_{PCA}	0.00	0.00	0.00	0.00	**0.01**
$Le_{PCA,\ winter}$	0.02	0.00	0.03	0.07	**0.10**

Tab. 14: r^2 values for apical shoot architecture (ROLOFF) related to PCA-derived indices: GF_{PCA}, Le_{PCA}, Lt_{PCA}, LAI_{PCA}, and $Le_{PCA,winter}$. The highest r^2 value in each row is highlighted.

Relationship to ALS-measurements

While the ALS-measured gap fractions were all significantly correlated to ROLOFF, nearly none of the relationships to the derived plant area index (L_{ALS}) for any of the crown parts was significant (Tab. 15). The highest r² values were achieved when only the first echoes of the ALS-measurement were considered (GF_{ALS} , r²=0.27, Fig. 25), differences between the two crown parts were marginal.

R² to ROLOFF	unweighted	All	F	F+L
GF_{ALS}	0.00	0.06	**0.27**	0.04
$GF_{ALS, lower}$	0.00	0.02	**0.25**	0.04
$GF_{ALS, upper}$	0.01	0.04	**0.23**	0.06
L_{ALS}	n.s.	n.s.	0.01	n.s.
$L_{ALS, lower}$	n.s.	n.s.	n.s.	n.s.
$L_{ALS, upper}$	0.00	0.02	n.s.	0.01

Tab. 15: r² values for apical shoot architecture (ROLOFF) related to ALS-derived gap fractions and plant area indices (different echo weightings): GF_{ALS}, $GF_{ALS, lower}$, $GF_{ALS, upper}$, L_{ALS}, $L_{ALS, lower}$, and $L_{ALS, upper}$. The highest r² value in each row is highlighted.

Relationship to TLS-measurements

All correlations of apical shoot architecture (ROLOFF) to TLS-derived quantities were significant. The gap fraction values were always better correlated to ROLOFF than the appertaining plant area index values (Tab. 16). The highest r² values were found for GF_{TLS} in the low resolution voxel model with an edge length of 50cm and a minimum point number per voxel of 2 (GF_{TLS}50_2, fig. 25). The relationship was a bit better for the lower 90% of the canopy than for the upper 10%. The minimum point number was not decisive, since also the voxel models with the same edge length and higher point numbers were similarly correlated to ROLOFF.

R² to ROLOFF	10_2	10_5	10_7	20_5	50_2	50_5	50_7
GF_{TLS}	0.07	0.24	0.25	0.33	**0.37**	0.37	0.36
$GF_{TLS, lower}$	0.05	0.22	0.23	0.30	**0.36**	0.35	0.35
$GF_{TLS, upper}$	0.00	0.19	0.17	0.23	**0.28**	0.25	0.25
L_{TLS}	0.00	0.00	0.00	0.06	0.13	**0.14**	0.13
$L_{TLS, lower}$	0.02	0.02	0.03	0.02	0.10	**0.10**	0.09
$L_{TLS, upper}$	0.00	0.01	0.01	0.04	**0.12**	0.10	0.09

Tab. 16: r² values for apical shoot architecture (ROLOFF) related to TLS-derived gap fractions and plant area indices (different voxel model resolutions): GF_{TLS}, $GF_{TLS, lower}$, $GF_{TLS, upper}$, L_{TLS}, $L_{TLS, lower}$, and $L_{TLS, upper}$. The highest r² value in each row is highlighted.

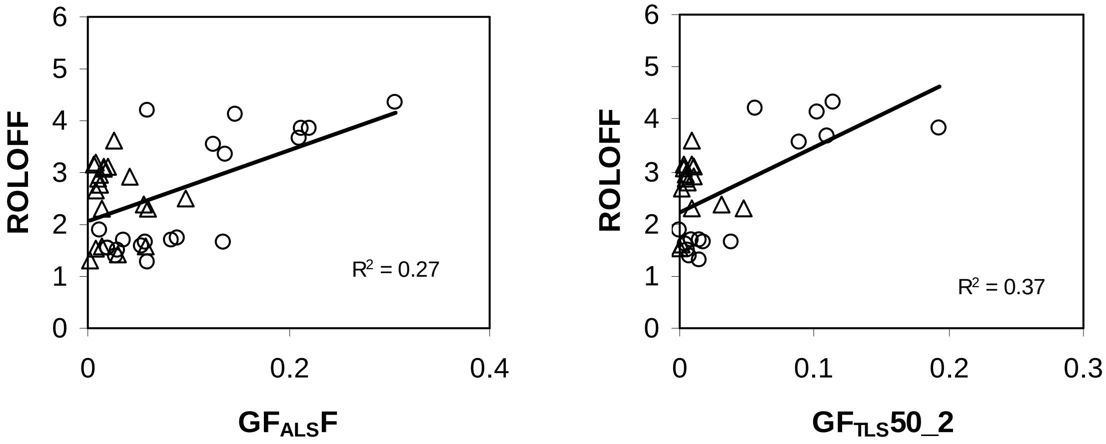

Fig. 25: Correlations of apical shoot architecture (ROLOFF) to gap fractions measured by airborne ($GF_{ALS}F$) and terrestrial lidar ($GF_{TLS}50\_2$). Oak stands are represented by open circles, beech stands by open triangles.

4.2.3 Fruiting

Fruiting, here defined as the proportion of trees with medium or high fucitification, was significantly correlated to all basic stand attributes, out of which the total stocks of wood (r^2=0.57) had the highest r^2 value. The height of the trees (r^2=0.52) was more important than the length of their shade canopy (r^2=0.49). Stand age (r^2=0.25) and LAI_L (r^2=0.26) could each only explain a quarter of the variability (Tab. 17, Fig. 26).

R^2 to…	Age of stand	Basal Area of stand	Height of trees	Length of shade canopy	Stocks of wood	LAI_L	Clumping Index
Fruiting	0.25	0.12	0.52	0.49	**0.57**	0.26	0.14

Tab. 17: r^2 values for Fruiting related to basic stand attributes including LAI_L and clumping index. The highest r^2 value is highlighted.

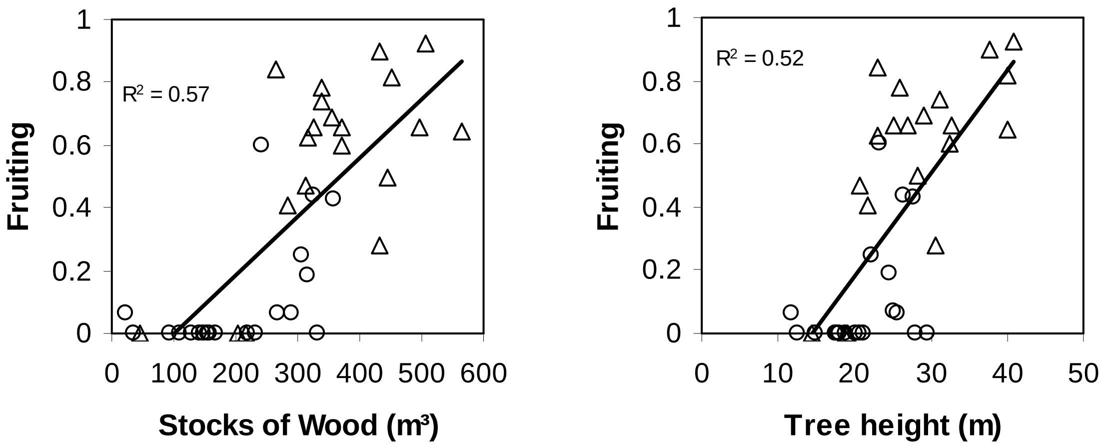

Fig. 26: Correlations of Fruiting to stocks of wood and tree height. Oak stands are represented by open circles, beech stands by open triangles.

Relationship to PCA-measurements

All PCA-derived quantities were significantly related to fruiting. While the winter measurements in the leafless stage had a very low r^2 value of up to 0.04, the summer measurements were the better correlated with fruiting the more they were corrected for clumping and woody surfaces (Tab. 18 and Fig. 27): $Le_{PCA}2$ had an r^2 -value of 0.28 and this increased to 0.45 after the correction for clumping ($Lt_{PCA}2$). The finally calculated $LAI_{PCA}2$ correlated the best with fruiting (r^2=0.48), in contrast to LAI_L , which explained less of the variability. From all possible opening angles, the narrow opening angle in which the 2 innermost rings of the PCA are evaluated correlated best, indicating that the data of larger opening angles that include a higher amount of shade canopy biomass could explain less of the variability in fruiting.

R^2 to Fruiting	Ring 1	Ring 2	Ring 3	Ring 4	Ring 5
GF_{PCA}	0.30	**0.31**	0.28	0.25	0.20
Le_{PCA}	0.22	**0.28**	0.27	0.25	0.23
Lt_{PCA}	0.39	**0.45**	0.45	0.43	0.41
LAI_{PCA}	0.40	**0.48**	0.47	0.46	0.46
$Le_{PCA,\ winter}$	0.02	0.02	**0.04**	0.03	0.03

Tab. 18: r^2 values for Fruiting related to PCA-derived indices: GF_{PCA}, Le_{PCA}, Lt_{PCA}, LAI_{PCA}, and $Le_{PCA,winter}$. The highest r^2 value in each row is highlighted.

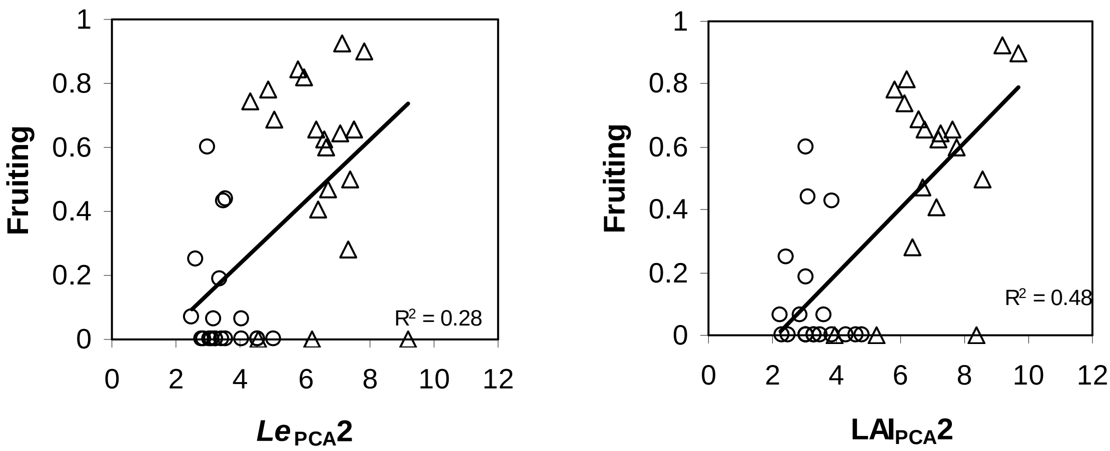

Fig. 27: Relationships of Fruiting to the uncorrected PCA measurement ($Le_{PCA}2$) and to $LAI_{PCA}2$, after the correction for clumping and woody surfaces. Oak stands are represented by open circles, beech stands by open triangles.

Relationship to ALS-measurements

Fruiting was not significantly correlated to some of the ALS-measured gap fractions, except in the case of the evaluation of only first echoes, where all correlations were significant. The highest correlations were found for GF_{ALS} and $GF_{ALS,lower}$ (r^2=0.38). The appertaining plant area indices (L_{ALS} and $L_{ALS,lower}$) were similarly correlated with r² values of 0.35 and 0.34, respectively. In all cases, the unweighted ALS-derived plant area index yielded the highest r² values.

R² to Fruiting	unweighted	All	F	F+L
GF_{ALS}	**0.38**	0.24	0.05	0.27
$GF_{ALS, lower}$	**0.38**	n.s.	0.04	n.s.
$GF_{ALS, upper}$	n.s.	n.s.	0.08	n.s.
L_{ALS}	**0.35**	0.25	0.26	0.09
$L_{ALS, lower}$	**0.34**	0.24	0.07	0.25
$L_{ALS, upper}$	**0.26**	0.22	0.11	0.23

Tab. 19: r² values for Fruiting related to ALS-derived gap fractions and plant area indices (different echo weightings): GF_{ALS}, $GF_{ALS, lower}$, $GF_{ALS, upper}$, L_{ALS}, $L_{ALS, lower}$, and $L_{ALS, upper}$. The highest r² value in each row is highlighted.

Relationship to TLS-measurements

Fruiting was not significantly correlated to a few of the TLS-derived gap fractions for the whole and for the lower canopy, which showed anyway low r² values in all resolutions of the voxel model (Tab. 20). On the other hand, the gap fractions for the upper 10% of the canopy were significantly correlated in all resolutions and reached r² values up to 0.45 ($GF_{TLS, upper}$50_7). The highest r² values in relation to fruiting were achieved for the TLS-derived plant area indices for the whole (L_{TLS}10_7, r² = 0.59) and for the lower canopy($L_{TLS,lower}$10_7, r² = 0.64, compare Fig. 28). Both plant area indices were best correlated in the high resolution voxel model with 10cm edge length. In total, there was no special resolution of the voxel model preferred.

R² to Fruiting	10_2	10_5	10_7	20_5	50_2	50_5	50_7
GF_{TLS}	**0.11**	n.s.	n.s.	0.09	0.05	0.06	0.06
$GF_{TLS, lower}$	**0.12**	n.s.	n.s.	0.11	0.05	0.06	0.06
$GF_{TLS, upper}$	0.00	0.36	0.34	0.44	0.37	0.43	**0.45**
L_{TLS}	0.00	0.54	**0.59**	0.23	0.16	0.20	0.21
$L_{TLS, lower}$	0.01	0.62	**0.64**	0.33	0.20	0.25	0.27
$L_{TLS, upper}$	0.02	0.01	0.01	0.00	**0.05**	0.04	0.04

Tab. 20: r² values for Fruiting related to TLS-derived gap fractions and plant area indices (different voxel model resolutions): GF_{TLS}, $GF_{TLS, lower}$, $GF_{TLS, upper}$, L_{TLS}, $L_{TLS, lower}$, and $L_{TLS, upper}$. The highest r² value in each row is highlighted.

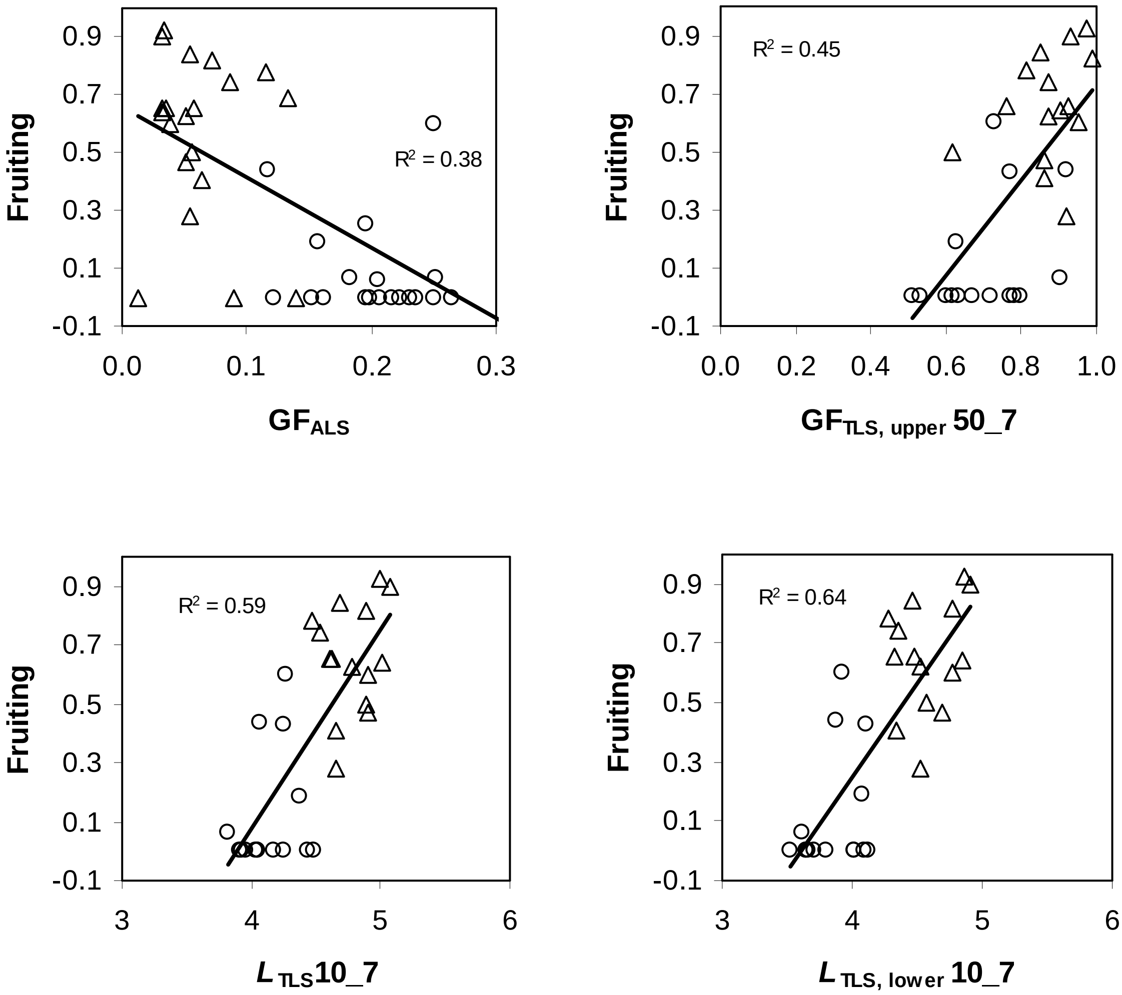

Fig. 28: Relationships of Fruiting to gap fractions derived from airborne (GF_{ALS}) and terrestrial ($GF_{TLS,upper}50\_7$) lidar – GF_{ALS} represents the whole canopy, $GF_{TLS,upper}50\_7$ only the upper 10% of it. Below this row are the correlations to the TLS-derived plant area indices $L_{TLS}10\_7$ and $L_{TLS,lower}10\_7$. Oak stands are represented by open circles, beech stands by open triangles.

4.2.4 Crown diameter related distance (CDRD)

CDRD was significantly correlated to all basic stand attributes and the highest r^2 value was found for the correlation to LAI_L (r^2=0.75, Fig. 29). Basal area explained 53% of the variability and all other basic stand attributes were only weakly correlated (r^2<0.14).

R² to…	Age of stand	Basal Area of stand	Height of trees	Length of shade canopy	Stocks of wood	LAI_L	Clumping Index
CDRD	0.04	0.53	0.02	0.01	0.03	**0.75**	0.13

Tab. 21: r^2 values for CDRD related to basic stand attributes including LAI_L and clumping index. The highest r^2 value is highlighted.

Relationship to PCA-measurements

CDRD was significantly related to all PCA-derived quantities. While the highest r^2values were achieved for the winter measurements of $Le_{PCA, winter}5$ ($r^2 = 0.55$, Fig. 29), the summer measurements were the worse correlated the more the initial measurement was changed by calculations and corrections: $GF_{PCA}4$ and $GF_{PCA}5$ reached an r^2 value of 0.52, which was reduced to 0.5 after conversion to $Le_{PCA}5$. The clumping correction of $Le_{PCA}4$ and $Le_{PCA}5$ produced $Lt_{PCA}4$ and $Lt_{PCA}5$, both with an r^2 value of only 0.34. Finally, the correction for woody surfaces produced an LAI_{PCA} that had an r^2 value of only 0.28 in the best correlated ring to CDRD ($LAI_{PCA}3$). In general, the higher opening angles (ring 4 and ring 5) that include larger parts of the lower canopy were better correlated to CDRD than the narrow opening angles.

R^2 to CDRD	Ring 1	Ring 2	Ring 3	Ring 4	Ring 5
GF_{PCA}	0.48	0.48	0.50	**0.52**	0.52
Le_{PCA}	0.40	0.45	0.47	0.48	**0.50**
Lt_{PCA}	0.28	0.32	0.34	**0.34**	0.34
LAI_{PCA}	0.24	0.28	**0.28**	0.27	0.24
$Le_{PCA, winter}$	0.11	0.25	0.47	0.55	**0.55**

Tab. 18: r^2 values for Fruiting related to PCA-derived indices: GF_{PCA}, Le_{PCA}, Lt_{PCA}, LAI_{PCA}, and $Le_{PCA,winter}$. The highest r^2 value in each row is highlighted.

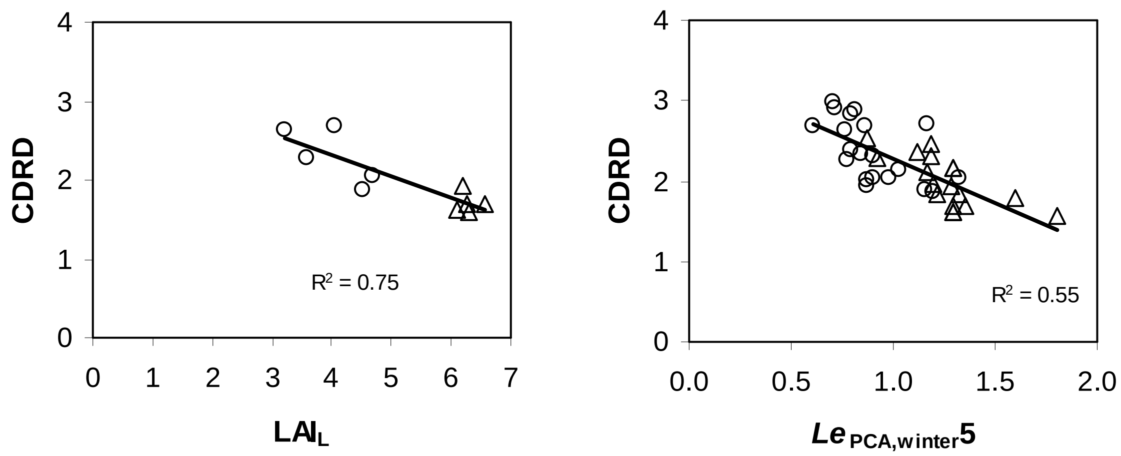

Fig. 29: Relationships of crown diameter related distance (CDRD) to litter trap measured LAI (LAI_L) and PCA-measured effective leaf area index measured in winter ($Le_{PCA,winter}5$). Oak stands are represented by open circles, beech stands by open triangles.

Relationship to ALS-measurements

The correlations of CDRD to L_{ALS} for the whole and for the lower canopy were not significant in most cases, except for the first echoes, while they were significant for the upper canopy, again except for the first echoes, which were not significantly correlated.

The highest r^2 values were reached in the relationship between CDRD and $L_{ALS,lower}F$ (r^2=0.63, Fig. 30) and also other r^2 values of the first echo evaluation were the highest in their category, including $GF_{ALS,lower}F$, which was the best correlated ALS-derived gap fraction value (r^2=0.62).

R^2 to CDRD	unweighted	All	F	F+L
GF_{ALS}	0.46	**0.60**	0.58	0.58
$GF_{ALS, lower}$	0.45	0.58	**0.62**	0.61
$GF_{ALS, upper}$	0.40	0.48	**0.50**	0.50
L_{ALS}	n.s.	n.s.	**0.50**	n.s.
$L_{ALS, lower}$	n.s.	n.s.	**0.63**	n.s.
$L_{ALS, upper}$	0.35	**0.44**	n.s.	0.42

Tab. 19: r^2 values for CDRD related to ALS-derived gap fractions and plant area indices (different echo weightings): GF_{ALS}, $GF_{ALS, lower}$, $GF_{ALS, upper}$, L_{ALS}, $L_{ALS, lower}$, and $L_{ALS, upper}$. The highest r^2 value in each row is highlighted.

Relationship to TLS-measurements

All correlations between CDRD and TLS-derived quantities were significant. The highest correlations were found between CDRD and the TLS-derived plant area index $L_{TLS}50\_7$ (r^2 = 0.8, Fig. 30). The gap fractions were best correlated in the medium resolution of the voxel model ($GF_{TLS}20\_5$, r^2 = 0.62). The good correlation of gap fractions and plant area indices for the whole canopy were in all cases not due to the upper 10% of the canopy (Tab. 20).

R^2 to CDRD	10_2	10_5	10_7	20_5	50_2	50_5	50_7
GF_{TLS}	0.00	0.44	0.39	**0.61**	0.55	0.58	0.59
$GF_{TLS, lower}$	0.00	0.46	0.42	**0.62**	0.55	0.58	0.59
$GF_{TLS, upper}$	0.01	0.05	**0.07**	0.03	0.00	0.01	0.01
L_{TLS}	0.06	0.43	0.39	0.70	0.73	0.78	**0.80**
$L_{TLS, lower}$	0.04	0.36	0.32	0.66	0.74	0.78	**0.79**
$L_{TLS, upper}$	**0.10**	0.08	0.08	0.05	0.06	0.05	0.04

Tab. 20: r^2 values for CDRD related to TLS-derived gap fractions and plant area indices (different voxel model resolutions): GF_{TLS}, $GF_{TLS,\,lower}$, $GF_{TLS,\,upper}$, L_{TLS}, $L_{TLS,\,lower}$, and $L_{TLS,\,upper}$. The highest r^2 value in each row is highlighted.

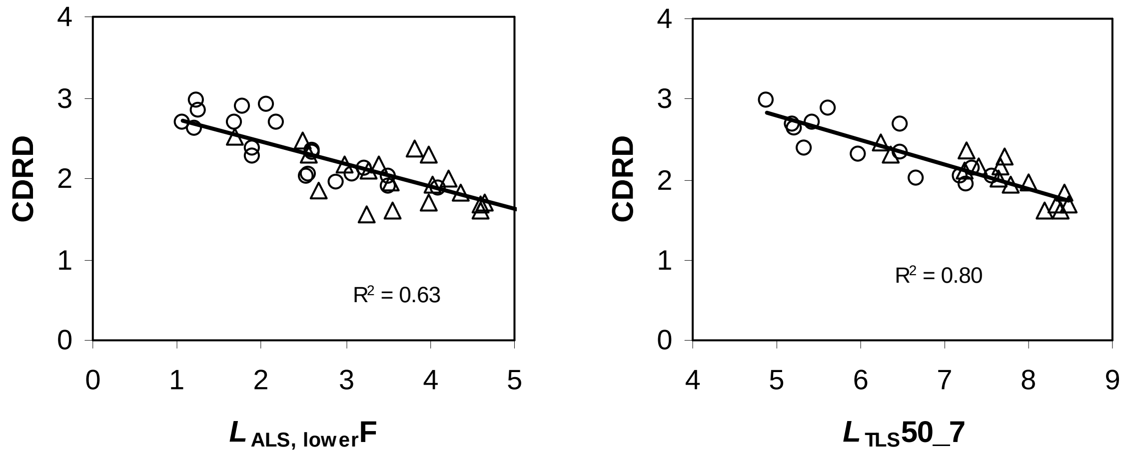

Fig. 30: Relationships of crown diameter related distance (CDRD) to plant area indices derived from airborne lidar ($L_{ALS,lower}F$) and from terrestrial lidar $L_{TLS}50\_7$. Oak stands are represented by open circles, beech stands by open triangles.

4.2.5 Fruiting corrected defoliation

The assessment of defoliation explicitly considers the visible fruits in a tree crown as non-foliage, thereby contributing to the defoliation value. In order to focus on the defoliation of non-fruiting trees, we therefore introduced a fruiting correction of the form:

$$\text{defoliation}_{FC} = \text{defoliation} * (1\text{-fruiting})$$

This means that a given defoliation is reduced whenever a certain amount of fruiting trees is involved and that it is reduced proportional to the amount of fruiting trees.

Fruitng corrected defoliation was significantly correlated to all basic stand parameters, but only litter trap measured LAI (LAI_L, $r^2 = 0.62$) and basal area (r^2=0.41) achieved relevant r^2 values.

R^2 to…	Age of stand	Basal Area of stand	Height of trees	Length of shade canopy	Stocks of wood	LAI_L	Clumping Index
defoliation_{FC}	0.05	0.41	0.01	0.01	0.03	**0.62**	0.02

Tab. 21: r^2 values for defoliation_{FC} related to basic stand attributes including LAI_L and clumping index. The highest r^2 value is highlighted.

Relationship to PCA-measurements

defoliation$_{FC}$ was significantly related to all PCA-derived quantities. The highest r² values were reached for the original gap fraction measurement of the PCA sensor (r²= 0.67, Fig. 31) and each step of further calculation and correction lowered the r² value: Logarithmic conversion to Le_{PCA} yielded a maximum r² of 0.5, clumping correction (Lt$_{PCA}$3) lead to an r² of 0.47, and the correction for woody surfaces resulted in an r² value of 0.45 in the best case (LAI$_{PCA}$3). The gap fraction measurement including the third ring yielded mostly the highest r² value (Tab. 22).

r² to Defoliation$_{FC}$	Ring 1	Ring 2	Ring 3	Ring 4	Ring 5
GF$_{PCA}$	0.66	0.62	**0.67**	0.67	0.62
Le_{PCA}	0.35	0.47	0.49	0.49	**0.50**
Lt_{PCA}	0.33	0.44	**0.47**	0.47	0.46
LAI$_{PCA}$	0.35	0.45	**0.45**	0.44	0.41
$Le_{PCA,\ winter}$	0.00	0.06	0.22	0.28	**0.33**

Tab. 22: r² values for defoliation$_{FC}$ related to PCA-derived indices: GF$_{PCA}$, Le_{PCA}, Lt_{PCA}, LAI$_{PCA}$, and $Le_{PCA,winter}$. The highest r² value in each row is highlighted.

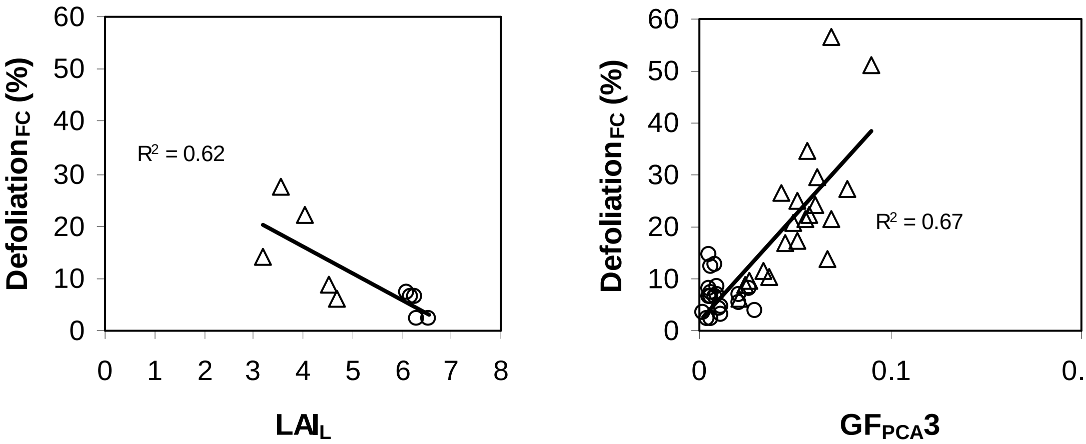

Fig. 31: Relationships of defoliation$_{FC}$ to litter trap measured LAI (LAI$_L$) and PCA-measured effective leaf area index measured in winter ($Le_{PCA,winter}$5). Oak stands are represented by open circles, beech stands by open triangles.

Relationship to ALS-measurements

All correlations between fruiting corrected defoliation and ALS-derived quantities were significant with p<0.01 (Tab. 23). The gap fractions were generally better correlated than the plant area indices, with a maximum r² for GF$_{ALS}$F+L (r²=0.56). The upper 10% of the canopy (GF$_{ALS,\ upper}$F+L, r²=0.55) contributed more to this result than the lower 90% (GF$_{ALS,lower}$F+L, r²=0.51). while the best results for ALS-derived gap fractions were achieved focusing on first and last echoes, the better results for plant area indices came from the first echoes (L_{ALS}F, $r^2=0.48$).

r^2 to **Defoliation$_{FC}$**	unweighted	All	F	F+L
GF_{ALS}	0.43	0.55	0.45	0.56
$GF_{ALS, lower}$	0.38	0.51	0.43	0.51
$GF_{ALS, upper}$	0.45	0.53	0.48	0.55
L_{ALS}	0.36	0.44	0.45	0.44
$L_{ALS, lower}$	0.34	0.41	0.43	0.41
$L_{ALS, upper}$	0.35	0.40	0.43	0.40

Tab. 23: r^2 values for Defoliation$_{FC}$ related to ALS-derived gap fractions and plant area indices (different echo weightings): GF_{ALS}, $GF_{ALS, lower}$, $GF_{ALS, upper}$, L_{ALS}, $L_{ALS, lower}$, and $L_{ALS, upper}$. The highest r^2 value in each row is highlighted.

Relationship to TLS-measurements

All correlations between defoliation$_{FC}$ and TLS-derived gap fractions and plant area indices were significant ($p<0.01$, Tab. 24). The derived plant area indices were in most resolutions better correlated than the appertaining gap fractions except for the high resolution (voxel edge length 10cm). The highest r^2 values were reached in the low resolution of 50cm voxel edge length (L_{TLS}50_7, $r^2=0.51$ and $L_{TLS,lower}$50_7, $r^2=0.49$). With respect to L_{TLS} and GF_{TLS}, the upper 10% of the canopy were much weaker correlated than the lower 90%.

r^2 to **Defoliation$_{FC}$**	10_2	10_5	10_7	20_5	50_2	50_5	50_7
GF_{TLS}	0.00	0.47	0.44	0.48	0.36	0.39	0.39
$GF_{TLS, lower}$	0.01	0.48	0.44	0.47	0.34	0.37	0.37
$GF_{TLS, upper}$	0.00	0.03	0.03	0.05	0.02	0.04	0.05
L_{TLS}	0.03	0.47	0.43	0.51	0.44	0.50	0.51
$L_{TLS, lower}$	0.02	0.39	0.34	0.48	0.43	0.48	0.49
$L_{TLS, upper}$	0.06	0.05	0.06	0.03	0.01	0.01	0.01

Tab. 24: r^2 values for Defoliation$_{FC}$ related to TLS-derived gap fractions and plant area indices (different voxel model resolutions): GF_{TLS}, $GF_{TLS, lower}$, $GF_{TLS, upper}$, L_{TLS}, $L_{TLS, lower}$, and $L_{TLS, upper}$. The highest r^2 value in each row is highlighted.

The best correlating gap fraction and plant area index derived from airborne and terrestrial lidar measurements are illustrated in Fig. 32.

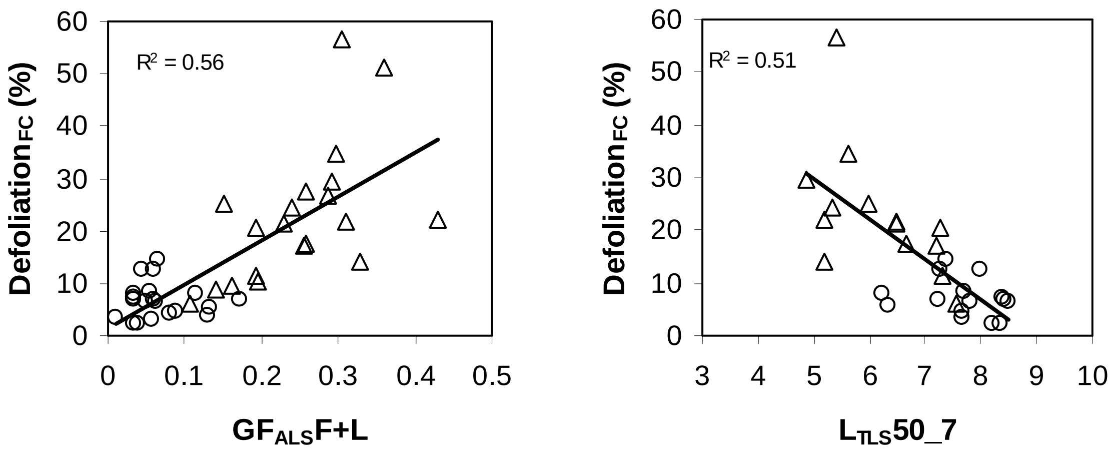

Fig. 32: Relationships of defoliation$_{FC}$ to ALS-derived gap fraction considering first and last echoes (GF$_{ALS}$F+L) and TLS-derived plant area index in a coarse resolution voxel model (L$_{TLS}$50_7). Oak stands are represented by open circles, beech stands by open triangles.

4.3 *Relationships between crown condition measurements*

The correlations between different measures of crown condition were all significant ($p<0.01$, Tab. 25). While Roloff and defoliation were to each other the best correlated crown condition measure ($r^2=0.59$), fruiting was not well correlated to any of the other measures. CDRD was best correlated to Defoliation$_{FC}$ ($r^2=0.51$), which had an inherently high r^2 value with defoliation ($r^2=0.57$).

r^2 to …	Defoliation	Roloff	Fruiting	CDRD	Defoliation$_{FC}$
Defoliation	1.00	**0.59**	0.03	0.42	0.57
Roloff	**0.59**	1.00	0.15	0.12	0.16
Fruiting	0.03	0.15	1.00	0.06	**0.23**
CDRD	0.42	0.12	0.06	1.00	**0.51**
Defoliation$_{FC}$	**0.57**	0.16	0.23	0.51	1.00

Tab. 25: r^2 values for the relationships between the different crown condition measures. The highest r^2 value in each row is highlighted.

The most important relationships between the investigated crown condition measures in our study are illustrated in Fig. 33.

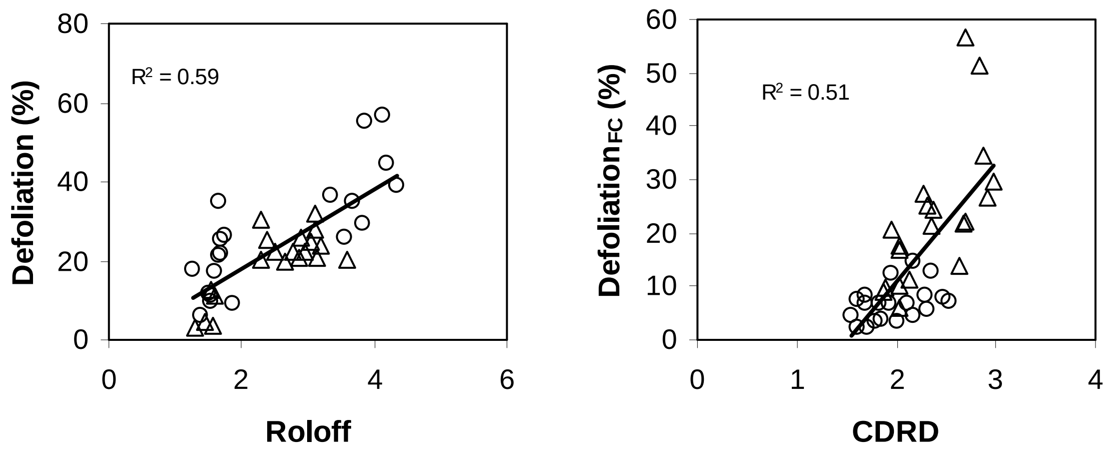

Fig. 33: Relationships between defoliation and apical shoot architecture (Roloff, left) and between fruiting corrected defoliation and crown diameter related distance (CDRD, right. Oak stands are represented by open circles, beech stands by open triangles.

5 *Conclusions*

5.1 *Summary of results and interpretations*

1. The narrow range of LAI values measured with litter traps on beech plots (LAI_L, Fig. 2) was a challenge for this investigation. With LAI values above 6, these plots were beyond the range that is believed to be measurable with the PCA-sensor (Gower et al. 1999). Anyway, the PCA-derived leaf area index LAI_{PCA} was excellently correlated with LAI_L (r^2=0.96, Fig. 3), indicating that even very small differences in gap fraction measurement are distinguished by the measurement method, allowing to measure LAI values up to 6 or 7 with the PCA.

2. After the correction for clumped leaf distribution and the contribution of woody surfaces, the PCA measured LAI was best correlated to LAI_L and showed the lowest root mean square error when four rings of the PCA-sensor were used (Fig. 4). In terms of bias, the third ring was better suitable than ring 4 (Fig. 5).

3. The uncorrected PCA measurement (Le_{PCA}) was as well correlated to LAI_L as the corrected LAI_{PCA}. The best choice in terms of r^2, RMSE, and bias was ring 3 (r^2 = 096, Figs. 7-9). A correction only for clumping (Lt_{PCA}) results in good correlations to ring 5.

4. Due to the very good agreement with LAI_L measurements, we accept $LAI_{PCA}4$, $LAI_{PCA}3$ and $Le_{PCA}3$ as ground truth measurements for the lidar derived plant area indices in order to have a larger number of plots to compare.

5. The ALS-derived plant area index L_{ALS} correlated very well with LAI_L (up to r^2=0.9). From the different evaluation methods, the unweighted L_{ALS} was the best choice for correlation with one of the LAI values (LAI_L, $LAI_{PCA}3$, and $LAI_{PCA}4$) while the weighted $L_{ALS}All$ correlated even a bit better to $Le_{PCA}3$ (r^2=0.93). The cause for this improvement lies probably in the similarity of the raw measurement methods, since gap fraction measurements through the canopy are evaluated by both methods. Anyway there is a physiologically relevant meaning in this high correlation coefficient, since $Le_{PCA}3$ was on its own very well correlated to LAI_L. For the evaluation of additional quantities, L_{ALS} has been used as proxy for the physiologically relevant LAI.

6. The first echoes related L_{ALS} measurement ($L_{ALS}F$) behaved in all relationships to PCA- or litter trap measured indices differently from the other L_{ALS} values and was always weaker correlated. On the other hand it showed better relationships to L_{TLS}, (up to r^2 = 0.9), defoliation (up to r^2=0.41), Roloff (up to r^2=0.27), and CDRD (up to r^2=0.63) than the other L_{ALS} values. Since it particularly evaluates signals from the upper canopy, it might more closely include that part of the canopy that is used in the crown condition assessments. The evaluation of this technique based on the current dataset still provides additional possibilities that could help to broaden our knowledge on crown condition measurements. Especially the more detailed evaluation of different echoes in the full waveform signal appears to be promising.

7. The TLS-derived plant area index L_{TLS} was very well correlated with LAI_L (r^2=0.86) and $Le_{PCA}3$ (r^2=0.81), when a high resolution voxel model was used. The correlation to $LAI_{PCA}3$ (r^2=0.79) and $LAI_{PCA}4$ (r^2=0.77) was a bit weaker but still very good. A large proportion of this good correlation is based on the distribution of woody biomass in space as may be seen in the relationship to the winter PCA-measurements ($LAI_{PCA,winter}$, Tab. 6, up to r^2=0.62).

8. The high resolution voxel model with an edge length of 10cm and a minimum point number of 7 per voxel ($L_{TLS}10\_7$) was best suitable as proxy for LAI and was also

well correlated to L_{ALS} (r^2=0.81). Since only a few resolutions have been evaluated in this investigation, the optimum might not yet have been achieved in the evaluation of this technique. Since it provides a 3D-model of the whole canopy, it might also help in a better evaluation of parts of the canopy wherever this is desirable, e.g. for defoliation and Roloff measurements.

9. While defoliation on its own reached in the best case an r^2 value of 0.44 (relationship to a TLS-derived gap fraction, GF_{TLS}20_5) and was only loosely correlated with any LAI-estimation, the fruiting corrected defoliation ($defolaition_{FC}$) reached higher correlations to LAI_L (r^2=0.62) and GF_{PCA}5 (r^2=0.67). This result is especially remarkable since the r^2 to the physiologically relevant LAI_L improved from 0.23 to 0.62 due to the fruiting correction.

10. Apical shoot architecture (ROLOFF) was by far best correlated to age of the stand (r^2=0.7), indicating that this quantitiy is not directly influenced by leaf area in the canopy but by the organisation of woody structures in space and the physiological stage of a tree crown. This result is also supported by the PCA-measurements Le_{PCA}, which are better correlated to ROLOFF in the winter than in the summer. The correlation between ROLOFF and defoliation might be attributed to the similar assessment scheme (selection of the same crown part) and the influence of fruiting on both quantities: The relationship to fruiting corrected defoliation is much weaker (r^2=0.16) than that to defoliation itself (r^2=0.59).

11. It may be physiologically explained that fruiting was well correlated to the stocks of wood (r^2=0.57) and to the height of trees (r^2=0.52). The correlation to LAI_L was weak on the other hand, eventually indicating that the carbon usage in fruit production does not strongly influence leaf production. Correlations to PCA-measurements were only in evaluations of 2 rings of the PCA-sensor remarkable (r^2 up to 0.48), probably since most fruits may be found in the upper part of the canopy. While ALS-measurements might be too coarse for the detection of fruits, the correlation to the highly resolved $L_{TLS,lower}$ 10_7 reached an r^2 of 0.64. It must be considered here that the lower canopy comprises 90% of total tree height so that the fruits visible from the ground are eventually more probably located in this part of the canopy than in the uppermost 10%.

12. CDRD was best correlated to $L_{TLS}50\_7$ ($r^2=0.8$), which is based on a rough model of crown structures and, therefore, similar to the measurement scheme of CDRD. While the correlation to LAI_L was good ($r^2=0.75$), the PCA-derived quantities were best suitable, if the measurements are performed in winter (r^2 up to 0.55), so that only woody structures are represented. These results support the principal independence of CDRD from leaf area in the canopy, though a strong relationship is inherent based on allometric relationships between crown diameters and leaf area.

13. Fruiting corrected defoliation was best correlated to LAI_L ($r^2=0.62$) and $GF_{PCA}3$ ($r^2=0.67$), which may be based on the natural correlation between the presence of leaves (LAI) and the relative absence of additional leaves (defoliation). It may also contribute to this result that the absence of leaves is visible as gaps in the canopy from below, which is only supported by the higher correlation to the ALS derived gap fraction ($GF_{ALS}F+L$, $r^2=0.56$) than to its plant area index.

5.2 *Recommendations*

A growing number of modelling approaches for forests relies on detailed assessments of the foliation status of the whole canopy. This includes models for the following processes:

- gas- and water exchange with the atmosphere
- soil hydrology
- element budgets
- deposition of nutrients and pollutants
- forest growth
- phenology
- forest vitality

It is the goal to make use of the possibilities offered by these modelling approaches for the purposes of the environmental monitoring program by providing reliable estimates of whole canopy foliation status.

The study at hand uses LAI measurement results derived from

a) leaf litter collections
b) LIDAR measurements (ALS and TLS)

for the assessment of whole canopy foliation status. The measurements were performed on 40 broadleaved forest stands in the federal state of Hesse. The 20 oak stands were between 15 and 203 years old, with a median age of 56, and the 20 beech stands ranged in age from 23 to

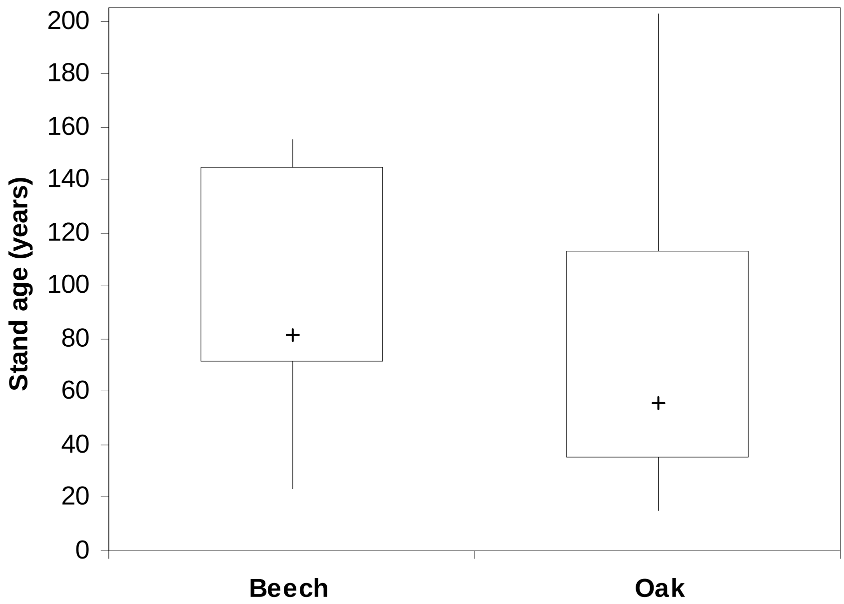

Fig. 34: Age distribution of the 40 investigated forest stands (20 beech and 20 oak stands). Shown are minimum, maximum, median value and interquartile range.

155 (median: 81.5, compare figure 34). The results are taken as independent LAI assessments (ground truth) against which the combined PCA and TRAC measurements are evaluated. Especially the performance of different opening angles and calculation methods for the PCA measurement is tested in order to enable best possible correspondence with the other methods.

With regard to this question, the favourite quantity derived from PCA measurements is the effective leaf area index based on 3 rings of the PCA sensor ($Le_{PCA}3$). This measurement was at least as well correlated to litter trap based LAI (LAI_L, r^2=0.96) as any corrected version of the directly measured effective LAI (e.g. total plant area index, Lt_{PCA}, and PCA-derived LAI, LAI_{PCA}), and it produces lower RMSE and bias values. Also, $Le_{PCA}3$ correlated best to both LIDAR derived plant area indices (L_{ALS} and L_{TLS}), with r^2 values of 0,93 (L_{ALS}) and 0,81 (L_{TLS}). The correction for the clumped distribution of leaves (leading to Lt_{PCA}) lowered the r^2 value in nearly all cases and the same was true for the correction for woody surfaces (leading to LAI_{PCA}).

Based on our measurement results and knowing that this result might not be valid for coniferous forests, where the degree of leaf clumping is higher, we recommend the following method for use of PCA measurements in Central European oak and beech stands:

1. Measurement of spatially averaged gap fractions according to the field protocol with either the PCA-sensor or digital hemispherical photography.
2. Calculation of the effective leaf area index for three rings of the PCA-sensor
3. No correction for clumping or the contribution of woody surfaces.
4. Optional: Collection of leaf litter samples for specific leaf area determination during the leaf fall period.

It still appears appropriate to us to gather further ground truth data on other forest stands in order to validate the result of this study. The remaining insecurity is due to the small differences between the different possible evaluation methods. But since they all point into the same direction, the efforts for additional TRAC or PCA winter measurements may not be justified from this study. We recommend the alternative use of digital hemispherical photography, because this measurement provides a permanent record of the stand leaf distribution. The photos provide the same information as the PCA measurements and may still be used after years to correct for the clumped distribution of leaves, whenever this is suggested by new results on the relevance of clumping correction. These new results can most easily be achieved by leaf sampling for specific leaf area determination along with litterfall collections, when PCA measurements or hemispherical photographs are taken in the same stand.

Our recommendation deviates from the field protocol in that only 3 rings of the PCA-sensor are used, with the effect that also smaller clearings are suitable for the above canopy reading. All other aspects with regard to PCA measurements are not affected.

Another deviation from the field protocol concerns hemispherical photography. Since not all available software programs enable the calculation of clumping indices, a program like the software hemisfer (Thimonier et al. 2010) or WinScanopy (Regent instruments inc.) is recommended. The use of hemispherical photography would also require further standardization in the field protocol.

The optional collection of litter samples for SLA determination during leaf litter collections is another deviation from the field protocol. All other aspects of the measurement methods are not affected.

6 References

Black, T.A., Chen, J.M., Lee, X.H., Sagar, R.M., 1991. Measuring leaf area index of plant canopies with branch architecture. Can. J. For. Res. 21, 1020-1028.

Bréda, N., Granier, A., 1996. Intra- and interannual variations of transpiration, leaf area index and radial growth of a sessile oak stand (Quercus petraea). Annales des Sciences Forestières 53, 521-536.

Bussotti, F., Borghini, F., Celesti, C., Leonzio, C., Cozzi, A., Bettini, D., Ferretti, M., 2003. Leaf shedding, crown condition and element return in two mixed holm oak forests in Tuscany, central Italy. Forest Ecology and Management 176, 273-285.

Chen, J.M., 1996. Optically-based methods for measuring seasonal variation of leaf area index in boreal conifer stands. Agricultural and Forest Meteorology 80, 135-163.

Chen, J.M., Black, T.A., 1992. Defining leaf area index for non-flat leaves. Plant, Cell and Environment 15, 421-429

Chen, J.M., Govind, A., Sonnentag, O., Zhang, Y.Q., Barr, A., Amiro, B., 2006.Leaf area index measurements at Fluxnet-Canada forest sites. Agricultural and Forest Meteorology 140 (1-4), 257-268

Chen, J.M., Rich, P.M., Gower, S.T., Norman, J.M., Plummer, S., 1997. Leaf area index of boreal forests: Theory, techniques, and measurements. Journal of Geophysical Research 102, 29429-29443.

Fleck, S., Mölder, I., Gebauer, T., Jacob, M., Jungkunst, H.F., Leuschner, C., 2011. Comparison of conventional 8-point canopy projections with lidar-based virtual canopy projections in a temperate old-growth forest. Annals of Forest Science, in press

Fleck, S., Mölder, I. 2011: LAI assessment with a voxel model based on multiple terrestrial laser scans, Annals of Forest Science, in prep.

Gower, S.T., Kucharik, C.J., Norman, J.M., 1999. Direct and Indirect Estimation of Leaf Area Index, fAPAR, and Net Primary Production of Terrestrial Ecosystems - a real or imaginary problem? Remote Sensing of Environment 70, 29-51.

Horntvedt, R., 1993. Crown density of spruce trees related to needle biomass. Forest Ecology and Management 59, 225-235.

Jonckheere, I., Fleck, S., Nackaerts, K., Muys, B., Coppin, P., Weiss, M. & Baret. F., 2004. A review of methods for leaf area index estimation of forest stands focused on digital hemispherical photography. Agricultural and Forest Meteorology 121(1), 19-35

Kersten, T., Sternberg, H., Mechelke, K., Lindstaedt, M., 2008. Datenfluss im terrestrischen Laserscanning - Von der Datenerfassung bis zur Visualisierung. In: Terrestrisches Laserscanning (TLS2008), Beiträge zum 79. DVW-Seminar am 6. und 7. November 2008 in Fulda. Schriftenreihe des DVW. Wißner-Verlag, Augsburg, pp. 31-56.

Leuschner, C., Voß, S., Foetzki, A., Meier, I.C., 2009. In welcher Beziehung stehen geschätzter Blattverlust und tatsächliche Blattflächenreduktion bei der Buche? Forstarchiv 80, 229-235.

LI-COR, inc. (Eds), 1992. LAI-2000 Plant Canopy Analyzer. Manual.

Mariano, G., Danson, F.M., Riano, D., Chuvieco, E., Ramirez, F. A., Bandugula, V. 2011. Terrestrial laser-scanning to estimate plot level forest canopy fuel properties. International Journal of Applied Earth Observation and Geoinformation 13(4), 636-645

Miller, J.B., 1967. A formula for average foliage density. A J B 15, 141-144.

Mizoue, N., Masutani, T., 2003. Image analysis measure of crown condition, foliage biomass and stem growth relationships of Chamaecyparis obtusa. Forest Ecology and Management 172, 79-88.

Monsi, S., Saeki, M., 1953. Über den Lichtfaktor in den Pflanzengesellschaften und seine Bedeutung für die Stoffproduktion. Japanese Journal of Botany 14, 22-52

Neuhaus, O., 1973. Die Waldgebiete Hessens (E Schönhals, Ed.). 17.

Paar, U., Dammann, I., Weymar, J., Wendland, J., Eichhorn, J., 2010. Waldzustandsbericht 2010 für Hessen. Nordwestdeutsche Forstliche Versuchsanstalt, Göttingen.

Smolander, H., Voipio, P., Kleinhenz, B., 2000. LAI-2000 estimates as an indicator of forest vitality. In: Forest condition monitoring in Finland - National report 1999. Research Papers. Metsäntutkimuslaitoksen tiedonantoja - The Finnish Forest Research Institute, pp. 79-89.

Solberg, S., Brunner, A., Hanssen, K.H., Lange, H., Næsset, E., Rautiainen, M., Stenberg, P., 2009. Mapping LAI in a Norway spruce forest using airborne laser scanning. Remote Sensing of Environment 113, 2317-2327.

Solberg, S., Næsset, E., Hanssen, K.H., Christiansen, E., 2006. Mapping defoliation during a severe insect attack on Scots pine using airborne laser scanning. Remote Sensing of Environment 102, 364-376.

Thimonier, A., Sedivy, I., Schleppi, P., 2010. Estimating leaf area index in different types of mature forest stands in Switzerland: a comparison of methods. European Journal of Forest Research 129, 543-562

Voll, H., 2001. 30 Jahre Waldbehandlung im Forsthydrologischen Untersuchungsgebiet Krofdorf. Wald und Wasser - 30 Jahre forsthydrologische Untersuchungen im Krofdorfer Forst 29, 30-40.

Zarnoch, S.J., Bechtold, W.A., Stolte, K.W., 2004. Using crown condition variables as indicators of forest health. Can J For Res 5, 1057-1070.